JOURNAL OF GEOPHYSICAL RESEARCH, VOL. 104, NO. C3, PAGES 3633–3653, FEBRUARY 20, 1999

Hydrocarbon measurements during tropospheric ozone depletion events: Evidence for halogen atom chemistry

B. Ramacher, J. Rudolph,[1] and R. Koppmann

Institut fur Atmosphärische Chemie (ICG-3), Forschungszentrum Jülich GmbH, Jülich, Germany

Abstract. During the Arctic Tropospheric Ozone Chemistry 1996 (ARCTOC 96) field campaign (March 29 to May 15, 1996), in situ measurements of C_2–C_8 hydrocarbons, selected C_1–C_2 halocarbons, and carbon monoxide were carried out at Ny Ålesund, Svalbard (78°55′N, 11°56′E). Two major tropospheric ozone depletions were observed during this period. In each case, concurrent depletion of alkanes and ethyne but no significant changes in benzene, chloromethane, or CO mixing ratios were detected. The change in the propane/benzene ratio can be used as evidence for the presence of chlorine radicals. Time integrated chlorine and bromine atom concentrations were calculated from the concentration changes of light alkanes and ethyne, respectively. At background ozone mixing ratios ($O_3 > 30$ ppbv) our calculations yielded no significant integrated halogen atom concentrations (Cl: $5 \pm 14 \times 10^8$ s cm^{-3}, Br: $9 \pm 42 \times 10^{10}$ s cm^{-3}). During major ozone depletion events, these values increase by more than a factor of 10 to values of about 10^{10} s cm^{-3} (Cl) and 5×10^{12} s cm^{-3} (Br). For such events the observed ozone losses can be explained quantitatively with these data. Our results show that free bromine atoms appear to be the major cause for ozone depletion (more than 92%). The contribution of chlorine atoms to the ozone loss is of the order of 1% or less. Highest integrated chlorine and bromine atom concentrations were found at lowest ozone mixing ratios and reached up to 1.4×10^{10} and 1.4×10^{13} s cm^{-3}, respectively. A closer analysis reveals that during each ozone depletion event the integrated chlorine atom concentration increases earlier than the integrated bromine atom concentration and remains at high levels for a longer period of time. The bromine atom concentration starts to increase when ozone mixing ratios are below 15–20 ppbv and reaches very high levels for ozone <5 ppbv. The integrated chlorine concentration appears to be anticorrelated to the ozone mixing ratio ($r^2 = 0.811$), whereas the integrated bromine concentration was found to be anticorrelated to the logarithm of the ozone mixing ratio ($r^2 = 0.895$).

1. Introduction

After the first observations by *Oltmans* [1981], the phenomenon of ozone depletion events in the arctic boundary layer during spring has been studied by several investigators [e.g., *Barrie et al.*, 1988; *Bottenheim et al.*, 1990; *Anlauf et al.*, 1994; *Solberg et al.*, 1996]. These depletion events are characterized by a sudden loss of ozone in the boundary layer. During spring, the ozone mixing ratio in the arctic troposphere usually ranges from 30 to 40 ppbv. Episodically however, it decreases within hours to very low values, sometimes even below the detection limit of about 1 ppbv. These events last for hours to days until the ozone mixing ratio increases as rapidly as it decreased. Frequently, ozone depletion was observed in air masses that were advected over ice- and snow-covered areas around the North Pole shortly before arriving at the measurement sites [*Hopper et al.*, 1994]. The height of the ozone-depleted air masses varies between 500 and 2000 m [*Anlauf et al.*, 1994; *Wessel*, 1997], depending on the height of the inversion layer. Ozone loss events are always associated with the existence of an inversion layer. From their duration and measured wind speeds, the spatial extent of these "tropospheric ozone holes" can be estimated to some hundred square kilometers. There are reasons to believe that the observed ozone losses are caused by the presence of significant concentrations of free halogen atoms in the depleted air masses [*Barrie et al.*, 1988; *Hausmann and Platt*, 1994; *Jobson et al.*, 1994; *Ramacher et al.*, 1997].

Although in the past there have been several intensive field studies, the chemical mechanism of the halogen-atom-induced ozone depletion is still not fully understood. Especially, the source of the halogen atoms is still unknown. The possibility of photolysis of halogenated organic trace gases has been studied, but none of the compounds examined yielded enough halogen radicals to account for the rapid ozone depletions [*Moortgat et al.*, 1993; *Yokouchi et al.*, 1994]. The most recent ideas concerning that topic have been published in a theoretical study by *Mozurkewich* [1995] and modeling studies by *Sander et al.* [1997] and by *Tang and McConnell* [1996]. They assume that halogen atoms are generated on aerosol particles, which is supported by an experimental aerosol study by *Kirchner et al.* [1997]. Still, the model calculations need to be confirmed by further experimental observations.

The purpose of this study was to verify and extend the database of nonmethane hydrocarbon (NMHC) mixing ratios collected during the Arctic Tropospheric Ozone Chemistry

[1]Now at Centre for Atmospheric Chemistry, York University, York, Ontario, Canada.

Paper number 1998JD100061.
0148-0227/99/1998JD100061$09.00

Table 1. Statistics of the VOC Mixing Ratios During ARCTOC 96, Detection Limits (dl), and Reproducibilities for VOC Measurements During ARCTOC 96

	Mixing Ratio/pptv								
Compound	Mean	Standard Deviation	Minimum	15% Percentile	Median	85% Percentile	Maximum	Detection Limit	Reproducibility, %
Ethane	1616	483	591	970	1655	2107	2485	26	3
Ethene	26	16	7	12	20	41	85	56	3
Ethyne	329	169	<dl	101	368	504	627	24	6
Propane	490	291	32	145	556	793	1116	25	3
Propene	<dl	<dl	<dl	<dl	<dl	<dl	17	21	5
2-methylpropane	74	55	5	16	73	133	212	9	3
n-butane	128	99	<dl	21	136	238	347	7	3
2-methylbutane	32	30	<dl	4	16	67	122	6	3
n-pentane	27	26	<dl	2	12	58	95	8	3
n-hexane	7	6	<dl	<dl	6	13	21	4	11
n-heptane	4	3	<dl	<dl	4	7	12	3	12
Benzene	102	36	51	63	88	144	188	11	4
Toluene	10	14	<dl	<dl	5	26	62	11	13
Ethylbenzene	2	1	<dl	<dl	2	3	6	3	8
Dimethylbenzenes	<dl	<dl	<dl	<dl	<dl	<dl	<dl	2	65
Ethanal*	111	53	32	061	101	170	307	45	20
2-propanone*	451	116	165	316	435	580	729	22	15
Chloromethane	528	21	473	507	529	546	627	17	8
Dichloromethane	46	2.4	42	44	46	50	58	1	5
Trichloromethane	27	6.3	15	20	26	34	43	1	13
Tetrachloromethane	138	2.6	132	135	139	141	145	0.2	7
1,1,1-trichloroethane	175	3.0	165	172	175	178	185	1	5
Tetrachloroethene	7.9	2.2	2.6	4.3	8.9	9.6	11.3	0.1	6
Bromomethane	13.7	1.5	10.6	12.2	13.4	15.5	17	0.2	39
Dibromomethane	1.1	0.08	0.9	1.1	1.1	1.2	1.3	0.2	40
Tribromomethane	0.65	0.25	<dl	0.4	0.6	0.7	1.9	0.1	63
Iodomethane	0.29	0.10	<dl	0.2	0.3	0.4	0.8	0.1	21

Detection limits were calculated for the mean preconcentrated sample volume.
*Lower limit; see methods.

1995 (ARCTOC 95) field campaign [*Ramacher et al.*, 1997] in order to provide more quantitative information for the suggested halogen-atom-induced tropospheric ozone depletions.

2. Methods

The experimental setup and the location of the measurement site will only be described briefly, since they have been published elsewhere [*Ramacher et al.*, 1997; *Ramacher*, 1997].

The ARCTOC 96 campaign was conducted at Ny Ålesund, Svalbard (78°55'N, 11°56'E) in spring 1996 (March 29 to May 15, 1996). Organic trace gases were measured by two in situ gas chromatographs. The first (GC1) was operated over the entire campaign and allowed the determination of C_2–C_8 hydrocarbons and C_1–C_2 halocarbons with a sampling frequency of 2 hours. Because of drifts in the electron capture detector response at the beginning of the experiment, halocarbon measurements began on April 6, 1996. With the second system (GC2), we determined C_2–C_7 hydrocarbons every 1.5 hours starting on April 2, 1996. Because of problems with the supply of liquid nitrogen, this system could not be operated continuously. CO was determined every 5 min by another in situ gas chromatograph operating between March 29 and May 15. All instruments were installed in the "Gruveverkstedet" building, which is only about 100 m away from where they had been placed during ARCTOC 95 [*Ramacher et al.*, 1997]. Thus no general difference in the mixing ratios of organic trace gases between both sites is expected, and data collected in both years are comparable. Both locations are about 1.5 km away from the village of Ny Ålesund. The road to Zeppelin Mountain was close to the measurement sites but not frequently used (<1 vehicle/h). Sample inlet and experimental setup were the same as in spring 1995 [*Ramacher et al.*, 1997].

Calibration of halocarbons and hydrocarbons was performed by comparison with daily measurements of an air standard of known composition. Its mixing ratios were of the order of several pptv to a few ppbv and thus comparable to those found in ambient air. Except for ethyne and halocarbons, for which the evaluation was based on a separate response factor, all hydrocarbon mixing ratios were calculated using a common carbon response factor (detection by flame ionization detector).

Detection limits range from 2 to 56 pptv, depending on the substance, the method, and the size of preconcentrated air sample. Reproducibilities (calculated from daily injections of a calibration gas) range from 2 to 65%, depending on the compound but were found to be lower than 10% for most compounds (Table 1). Extremely poor reproducibilities were found for dimethylbenzenes (65%), iodomethane (21%), and bromomethanes (39–63%). In the case of dimethylbenzenes, this is due to incomplete separation of the compounds from 2-propanone, which produces a significantly higher signal than the dimethylbenzenes when analyzing the calibration air. The poor reproducibilities for the iodomethanes and bromomethanes are probably caused by adsorption of these compounds on the inner walls of the calibration air cylinder, since much better reproducibilities were found when comparing consecutive air samples or when air from a diffusion device used for calibration purposes was injected [*Gautrois*, 1996]. Although the en-

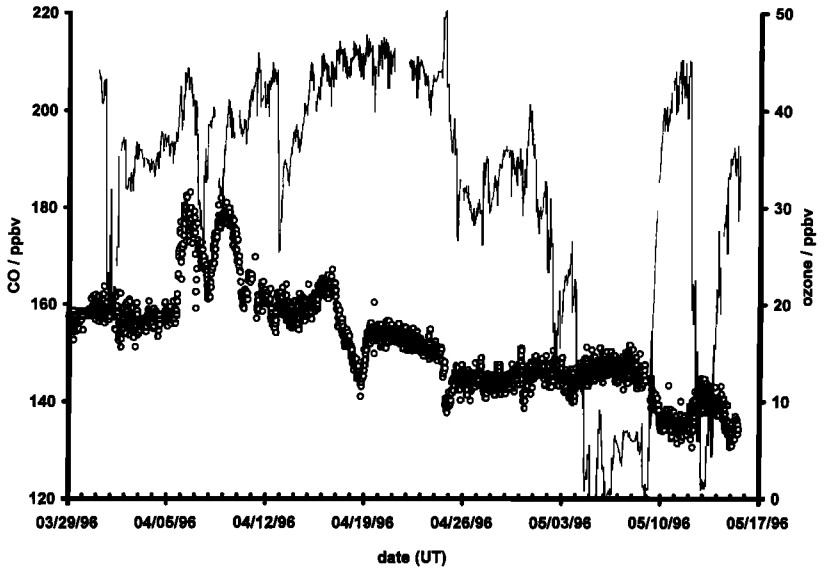

Figure 1. Time series of carbon monoxide and ozone mixing ratios during ARCTOC 96: solid line, ozone [*Arnold et al.*, 1997]; circles, CO (30 min mean).

tire sample inlet and preconcentration system of the gas chromatographs is made of stainless steel, which is supposed to cause problems when analyzing oxygenated compounds [*Leibrock*, 1996], the reproducibilities of ethanal and 2-propanone were surprisingly good. From the daily injections of the calibration gas, we calculated them to be 20% for ethanal and 15% for 2-propanone. In a series of 10 consecutive air samples, we even found mean reproducibilities of about 16% and 8%, respectively. The absolute mixing ratios of both compounds are quite uncertain, since they were calculated from the flame ionization detector's (FID's) mean carbon response, which leads to an underestimation of the corresponding mixing ratios of the order of a factor of 3 (ethanal) and factor of 2 (2-propanone) [*Sternberg et al.*, 1962]. However, that might also depend on the operating conditions (e.g., detector temperature, gas flows).

As we have shown in a previous publication [*Ramacher et al.*, 1997] the two different gas chromatographic systems for the determination of hydrocarbons give very similar results. During ARCTOC 96, we had a total of 88 simultaneous measurements for which we compared the median ratio (GC1/GC2) of the results. Very good agreement was found for ethane (0.98), ethyne (1.00), propane (1.02), 2-methylpropane (1.01), n-butane (1.03), n-pentane (0.97), and benzene (0.97). In the cases of n-heptane, propene, and ethene, all simultaneous measurements were below the instruments' detection limit, and such a comparison would not be meaningful. For 2-methylbutane and n-hexane the results determined with GC1 were always lower than with GC2. The mean differences between both methods were 8 pptv for 2-methylbutane and 7 pptv for n-hexane. A possible reason for this behavior might be incomplete chromatographic separations on GC1, which may result in an inadequate peak area definition (peak overlap for 2-methylbutane/1,1-dichloroethene and n-hexane/trichloromethane). However, in the case of n-hexane we could just compare three simultaneous measurements above the detection limit. Because of the good comparability of the two different methods, the data sets were combined for the further analyses of the hydrocarbon data, except for 2-methylbutane.

The measurements of carbon monoxide were conducted by using a reduction gas analyzer (RGA3, Trace Analytical, Inc.). A reference air of known CO mixing ratio and the sample were measured alternately in order to compensate for possible drifts in the detector response. Since the time needed for one determination was about 2.5 min, a sample was analyzed every 5 min. The detection limit and the reproducibility were calculated to 7 ppbv and 1.1%, respectively. The linearity of the CO in situ instrument was checked prior to the field experiment. The response was found to be linear for CO mixing ratios up to about 560 ppbv [*Ramacher*, 1997].

3. Results

3.1. Carbon Monoxide Determination

Figure 1 shows a time series of carbon monoxide and ozone mixing ratios during the ARCTOC 96 campaign. The ozone data were obtained at the site by *Arnold et al.* [1997]. Infrequently, we observed outliers in the CO data set. Those had always higher mixing ratios than background air and were removed from the CO data set, since they reflected interference of local sources like skidoos, cars, or fossil fuel combustion from the village's power generator station. This was confirmed by increased NMHC mixing ratios in samples collected simultaneously or by observations of cars or skidoos passing upwind of the measurement site. The CO mixing ratio decreased from about 160 ppbv in late March to some 130 ppbv in mid-May. Maximum CO mixing ratios reached 188 ppbv between April 5 and 9, 1996.

Several ozone depletion events were encountered during the field experiment. During minor ozone depletion events on April 1 and 12, no significant changes of the CO mixing ratio were found. During the minor depletion periods on April 7–8, the CO mixing ratio was highly variable but showed no correlation to ozone. During the major ozone depletion event on May 4–9, the CO mixing ratio was constant at about 145 ppbv. After that, it varied between 130 and 142 ppbv and was anticorrelated to the ozone mixing ratio.

3.2. VOC Time Series

The time series of selected organic trace gas mixing ratios are depicted in Figure 2. Statistical data on the mixing ratios of all monitored volatile organic compounds (VOCs) is given in Table 1. Ethane and propane were the only compounds present at mixing ratios exceeding 1 ppbv. None of the other monitored organic trace gases except 2-propanone and ethyne ever exceeded mixing ratios of 500 pptv. Propene and dimethylbenzene mixing ratios were always below the detection limits of 20 and 2 pptv, respectively. For most compounds, i.e., alkanes, aromatics, ethyne, ethene, ethanal, dichloromethane, and tetrachloroethene, mixing ratios decreased with time. The concentrations of chloromethane, 1,1,1-trichloroethane, tetrachloromethane, and dibromomethane remained almost constant throughout the entire measurements. Bromomethane and 2-propanone mixing ratios increased during the study, with average rates of 0.1 and 4 pptv/d, respectively. As for CO, the highest mixing ratios of most of the hydrocarbons were observed between April 5 and 9, 1996.

However, the most dominant feature was the change in VOC pattern during the ozone depletion events, especially during the major depletion periods in May 1996. Alkanes, ethyne, and tetrachloroethene mixing ratios were well correlated with the ozone mixing ratio during the depletion events. The changes of the mixing ratios of aromatics, other halocarbons (except tribromomethane), ethene, ethanal, and CO were smaller than their variability at background ozone mixing ratios. Both 2-propanone and tribromomethane appear to be anticorrelated to ozone during these periods.

3.3. Calculation of Time Integrated Halogen Atom Concentrations

The changes in VOC pattern in ozone depleted air can be used to calculate time integrated halogen atom concentrations [*Jobson et al.*, 1994; *Solberg et al.*, 1996; *Ramacher et al.*, 1997]. The basic assumption for this calculation is that the difference between the VOC mixing ratios in ozone-depleted air masses and during "normal" ozone conditions was caused solely by halogen atoms. Then the second-order loss of VOC with halogen atoms can be rearranged to (1) and (2) to calculate time integrated chlorine and bromine atom concentrations [*Ramacher et al.*, 1997]. Time integrated chlorine atom concentrations can be calculated from the changes in alkane mixing ratios. Because of the very slow reaction between alkanes and bromine atoms, even the presence of large amounts of bromine atoms will not affect the alkane concentrations. The bromine atom concentration can be calculated from the change in ethyne after correction for the Cl-atom-induced change. Ethyne is the only compound reacting with bromine atoms at a significant rate, which could be determined with sufficient accuracy. Since the time of the injection of halogen atoms into the air mass (t_0) is not known, the integrals are indefinite.

The rate constants for the reactions between hydrocarbons and halogens can be found in the literature (Table 2). The alkane and ethyne concentrations during the ozone depletion events were measured. The only unknowns that remain are the initial alkane or ethyne concentrations, i.e., the concentration of these compounds before halogen atoms were injected into the air masses. Following previous arguments [*Ramacher et al.*, 1997; *Ramacher*, 1997], we interpolated the mixing ratios determined at normal ozone levels (defined as ozone >30 ppbv) before and after the depletion event by an exponential least squares fit. Those values were used as an estimate for the initial alkane or ethyne concentration [alkane/ethyne]$_0$:

$$-\int_{t_0}^{t_x} [\mathrm{Cl}]\, dt = \frac{1}{k_{\mathrm{alkane,Cl}}} \ln\left(\frac{[\mathrm{alkane}]_x}{[\mathrm{alkane}]_0}\right) \tag{1}$$

$$-\int_{t_0}^{t_x} [\mathrm{Br}]\, dt = \frac{1}{k_{\mathrm{C_2H_2,Br}}}\left(\ln\left(\frac{[\mathrm{C_2H_2}]_x}{[\mathrm{C_2H_2}]_0}\right) + k_{\mathrm{C_2H_2,Cl}}\int_{t_0}^{t_x} [\mathrm{Cl}]\, dt\right) \tag{2}$$

where $\int [X]\, dt$ is the time integrated halogen atom concentration (X = Cl, Br), $[Y]_{X/0}$ is the concentration of compound Y (Y = alkanes, ethyne) during ozone depletion (subscript X) and in background air (subscript 0), $t_{X/0}$ is the time of the measurement (subscript X) and time of the injection of halogen atoms into the air mass (subscript 0), and $k_{Y,X}$ is the rate constant for the reaction between halogen atoms (X = Cl, Br) and VOC (Y = alkanes, ethyne).

We used an exponential fit for the interpolation, since mixing processes as well as the removal by OH radicals are following an exponential relationship. In contrast to the ARCTOC 95 campaign [*Ramacher et al.*, 1997], no reasonable interpolations covering the whole campaign could be found. Therefore two separate interpolations were used: one for the minor ozone depletion event (March 31 to April 2, 1996) and a second for the major depletions in May 1996 (Figures 3a and 3b). Unfortunately, no additional data are available from the measurement site covering a longer time interval during spring 1996. Thus seasonal trends of the organic trace gases that could serve to calculate "background mixing ratios" could not be determined.

The error of the time integrated halogen atom concentration depends on the precision of the measurements, the accuracy of the estimate of the initial trace gas concentration, and the accuracy of the rate constants.

The uncertainty of the initial hydrocarbon concentrations was estimated from the mean deviation between the exponential fits and the measured values at ozone mixing ratios exceeding 30 ppbv. Depending on the compound, these uncertainties vary from 3% to 19%.

Another way of assessing the uncertainty of the initial hydrocarbon concentrations is to look at the uncertainty of the fit itself, which can be calculated from the errors in slope and intercept. We found that both methods lead to very similar results (difference in the estimated uncertainties <1%) for the period between April 18 and May 15, which includes the two major ozone depletion events in May 1996. For the minor depletion period (March 31 to April 5) the uncertainty estimated from the mean deviation between the fitted and measured values is significantly lower (by 16–63%) than that estimated from the errors of the fitting procedure. We think that the latter method yields unrealistic estimates. In the case of ethyne, for example, the uncertainty of the initial concentration would be about 77%. This is much larger than the variability of the measurements during that period of time (44%). The method we chose yields an uncertainty of 14% for that case, which is slightly larger than the relative standard deviation of the ethyne mixing ratios measured during that period of time (11%).

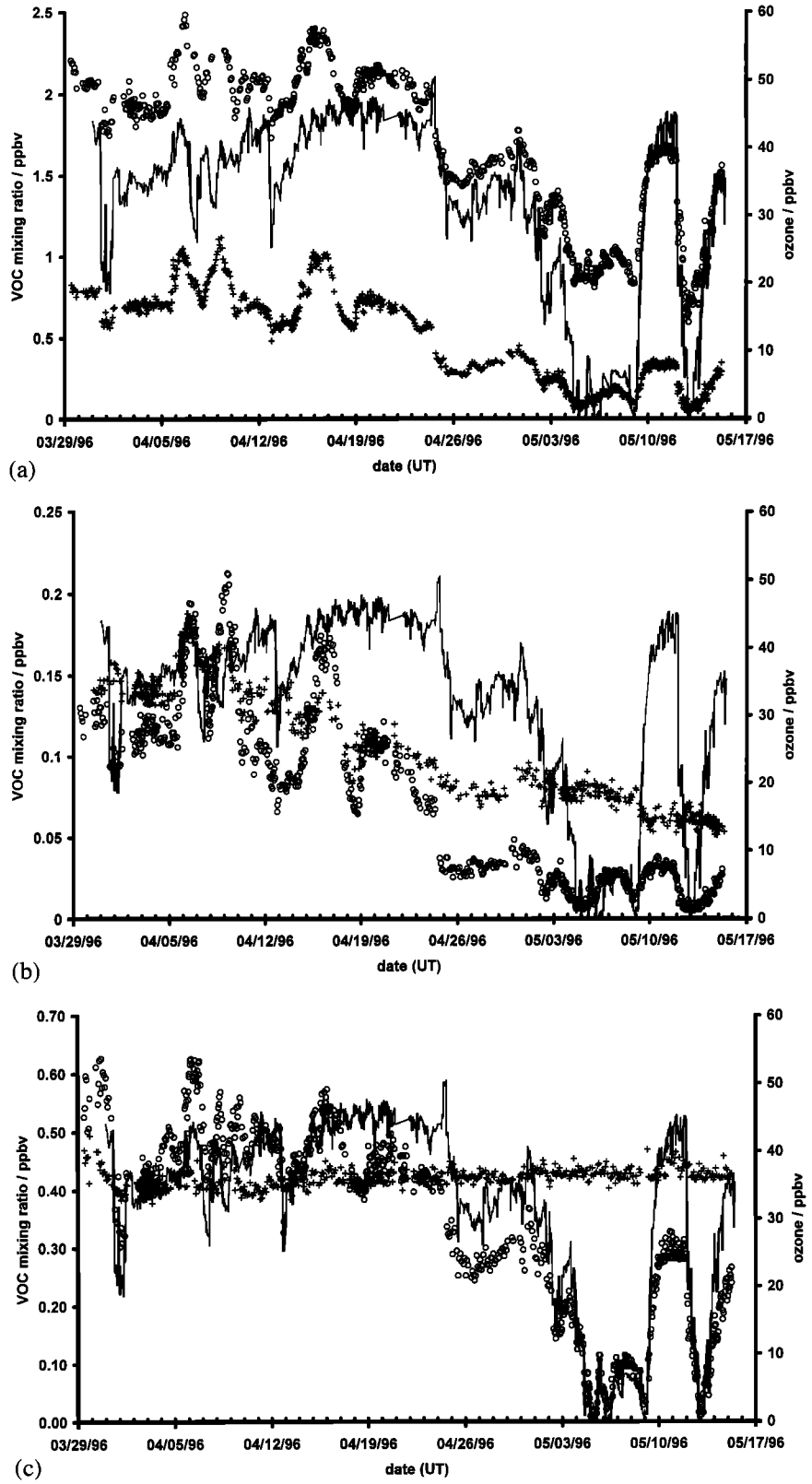

Figure 2. Time series of organic trace gas mixing ratios during ARCTOC 96. Solid line in all figures represents ozone [*Arnold et al.*, 1997], (a) circles, ethane; crosses, propane; (b) circles, 2-methylpropane; crosses, benzene; (c) circles, ethyne; crosses, chloromethane; (d) circles, tetrachloroethene/10; crosses, tribromomethane; and (e) circles, 2-propanone; crosses, ethanal (lower limits; see methods).

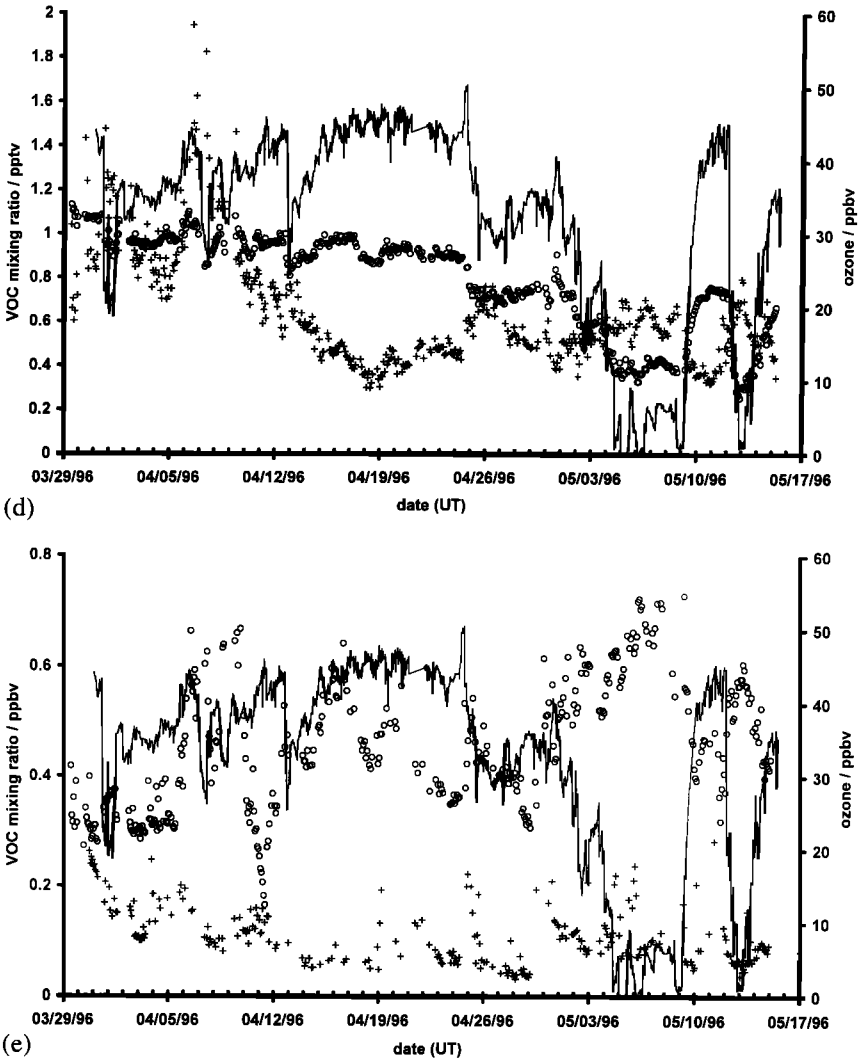

Figure 2. (continued).

The uncertainties of the rate constants are reported in the references cited in Table 2 and found to be 17% for $k_{\text{ethane,Cl}}$, 71% for $k_{\text{propane,Cl}}$, 15% for $k_{\text{2-methylpropane,Cl}}$, 11% for $k_{\text{n-butane,Cl}}$, 31% for $k_{\text{ethyne,Cl}}$, ~40% for $k_{\text{ethyne,Br}}$, 23% for $k_{\text{ozone,Cl}}$, and 25% for $k_{\text{ozone,Br}}$. The large error of the rate constant $k_{\text{propane,Cl}}$ results from a rather conservative estimate of the temperature dependence. *Atkinson and Aschmann* [1985] claim that the temperature dependence is weak. Their value for the rate constant at 298 K is $1.34 \pm 0.16 \times 10^{10}$ cm^3 s^{-1}, which is just 5% off the rate constant at 250 K used here. It has to be pointed out that the rate constants of the butanes with Cl are only given for 298 K. Using them at 250 K might add a systematic error to the uncertainty given above.

Table 3 summarizes typical time integrated halogen atom concentrations calculated for different ozone depletion events in spring 1996 together with some meteorological data. Based on changes in the mixing ratios of ethane, propane, 2-methylpropane, and n-butane during major ozone depletion periods (May 4, 5, and 13), time integrated chlorine atom concentrations exceeding 10^{10} s cm^{-3} were calculated. For these events the agreement is good between the integrated chlorine atom concentrations calculated on the basis of individual alkane concentration changes. The standard deviations of the mean integrated chlorine atom concentrations ($1.3–2.4 \times 10^9$ s cm^{-3}) are smaller than the uncertainties of the integrated chlorine atom concentrations calculated on the basis of individual alkane concentration changes ($2.4–9.8 \times 10^9$ s cm^{-3}). The same holds true for the integrated bromine atom concentrations calculated for these periods. The mean integrated bromine atom concentrations are about 1000 times larger than the integrated chlorine atom concentrations and varied between 6.4×10^{12} and 11.4×10^{12} s cm^{-3}, with standard deviations ranging from 0.6 to 1.2×10^{12} s cm^{-3}. The uncertainty of integrated bromine atom concentrations calculated on the basis of concentration changes of an alkane/ethyne pair is of the order of $3.6–6.7 \times 10^{12}$ s cm^{-3}.

For May 6 and 8, the integrated chlorine atom concentrations calculated from the changes in different alkanes varied between 2.4×10^9 and 12.0×10^9 s cm^{-3} (May 6) and 1.2×10^9 and 9.7×10^9 s cm^{-3} (May 8). These large deviations cannot be explained by the uncertainties of the integrated chlorine atom concentrations calculated from the changes in single alkanes ($0.6–5.1 \times 10^9$ s cm^{-3}). However, this did not strongly affect the calculation of integrated bromine atom concentrations. The mean integrated bromine atom concentrations of 10.9×10^{12} s cm^{-3} (May 6) and 4.6×10^{12} s cm^{-3}

Table 2. Rate Constants for the Reaction of VOC + $X \rightarrow$ products (X = OH, Cl, Br)

Compound	k(OH)		k(Cl)		k(Br)		k(Cl)	k(Br)
	10^{-14} cm^3 s^{-1}		10^{-14} cm^3 s^{-1}		10^{-14} cm^3 s^{-1}		k(OH)	k(OH)
CO	23.6	b[6]	7.2	b[6]			0.3	
Chloromethane	2.16	b[1]	3.6	a[5]			1.7	
Dichloromethane	5.7	b[6]	14.0	b[6]			2.5	
Trichloromethane	5.46	b[6]	4.1	b[6]			0.8	
Trichloroethane	0.37	b[6]	0.2	a[6]			0.5	
Bromomethane	1.12	b[6]	25.5	b[13]			22.8	
Dibromomethane	6.6	b[6]	19.3	b[13]			2.9	
2-propanone	15.4	b[1]	350	a[1]			22.7	
Ethanal	1,650	b[6]	7,200	a[1]	308	b[1]	4.4	0.19
Methane	0.21	b[1]	4.3	b[1]			20.6	
Benzene	91.1	b[2]	0.9	a[15]	<1	a[14]	0.009	<0.01
Ethane	13.2	b[1]	5,370	b[6]	0.00001	a[14]	406.8	≪0.01
Ethene	1,110	b[2]	9,290	a[8]	16.0	a[11]	8.4	0.01
Ethyne	53.3	b[6]	7,350	b[6]	15.4	b[11]	137.9	0.29
Propane	75.6	b[1]	14,100	b[6]	0.0043	a[14]	186.5	≪0.01
Propene	3,000	b[3]	32,200	a[8]	270	a[14]	10.7	0.09
2-methylpropane	193	b[4]	15,100	a[8]	0.14	a[14]	78.2	≪0.01
n-butane	199	b[4]	19,700	a[7]	0.007	a[14]	99.0	≪0.01
2-methylbutane	390	a[2]	20,200	a[7]			51.8	
n-pentane	405	b[2]	20,200	a[7]			49.9	
n-hexane	557	a[2]	30,200	a[7]			54.2	
n-heptane	720	a[2]	34,000	a[7]			47.2	
Toluene	758	b[2]	5,890	a[7]	<1	a[14]	7.8	≪0.01
Tetrachloroethene	7.72	b[2]	4,610	b[10]	0.009	a[16]	597.2	0.001
Ozone	3.10	b[2]	966	b[3]	67.7	b[9]	311.6	21.8

According to arctic conditions, data are given for 250 K whenever possible. Where temperature dependence is unknown, data at 298 K are given. Data are those recommended by NIST or JPL publication 97-4 [*DeMore et al.*, 1997]. Values followed by letter a are data at 298 K, and b are at 250 K.

References are 1, *Atkinson et al.* [1992]; 2, *Atkinson* [1986]; 3, *Atkinson et al.* [1989]; 4, *Atkinson* [1994]; 5, *Taylor et al.* [1993]; 6, *DeMore et al.* [1997]; 7, *Atkinson and Aschmann* [1985]; 8, *Wallington et al.* [1988]; 9, *Nicovich et al.* [1990]; 10, *Nicovich* [1996]; 11, *Barnes et al.* [1993]; 12, *Atkinson and Aschmann* [1987]; 13, *Tschuikow-Roux et al.* [1988]; 14, *Bierbach et al.* [1996]; 15, *Arnya* [1996]; 16, *Ariya et al.* [1997].

(May 8) are within the uncertainties of the values calculated from the changes in different alkane/ethyne pairs.

In the case of minor ozone depletions as observed on April 1, April 26, and May 2, the time integrated chlorine atom concentrations were 2.0, 4.9, and 6.6 $\times$ 10^9 s cm^{-3}, respectively. The time integrated bromine atom concentrations for these periods were 2.1, 0.2, and 1.9 $\times$ 10^{12} s cm^{-3}, respectively. Although the relative change in the hydrocarbon mixing ratios during these events was smaller than on May 6 and 8, the mean integrated halogen concentrations are well within the uncertainties of the integrated concentrations calculated from the changes in individual alkanes and alkane/ethyne pairs.

The errors of the integrated chlorine atom concentrations calculated from changes in single alkanes are around 20–30%. As stated above, the errors of the rate constants for the reaction between alkanes and chlorine atoms, the error of the measured alkane concentration, and the uncertainty of the initial alkane concentration contribute to the error of the integrated chlorine atom concentration. At high integrated chlorine atom concentrations this value is dominated by the error of the rate constants. Except for propane, for which the uncertainty of the rate constant is very large (71%), the different uncertainties contribute about equally to the error of the integrated chlorine atom concentration calculated for minor ozone depletions.

The errors of the time integrated bromine atom concentrations are always larger than those of the integrated chlorine atom concentrations and much more variable (45–110% during substantial ozone depletions). The error of the ethyne determination, the estimate of the initial ethyne concentration, and the error of the rate constant between ethyne and bromine atoms contribute about equally to this large relative error of the time integrated bromine atom concentration. The contributions of $\Delta k_{\text{ethyne,Cl}}$ and $\Delta \int [\text{Cl}]\, dt$ become more important at lower ozone mixing ratios.

4. Discussion

4.1. Time Series of CO and Organic Trace Gases

The decrease in concentration with time, which was found for a number of organic trace gases in this study, was also observed during the ARCTOC 95 experiment [*Ramacher et al.*, 1997]. It is part of the seasonal trend seen for most organic trace gases throughout the entire arctic troposphere [*Beine et al.*, 1996; *Jobson et al.*, 1994; *Solberg et al.*, 1996]. It is explained by transport processes and photochemistry [*Barrie*, 1986].

Most VOC reached highest mixing ratios between April 5 and 9, 1996. During this period, polluted air masses from the Eurasian continent were advected to the measurement site. This can be seen from trajectory analyses calculated by the Danish Meteorological Institute's high resolution limited area model (HIRLAM) (A. Rasmussen, private communication, 1997) as well as other trace gas and aerosol data collected during ARCTOC 96 (R. Staebler, private communication, 1996). Two minor ozone depletions were observed during this period (April 7–8). These will not be further analyzed because the trace gas loading of the polluted air masses is not comparable to that found at any other time during the campaign.

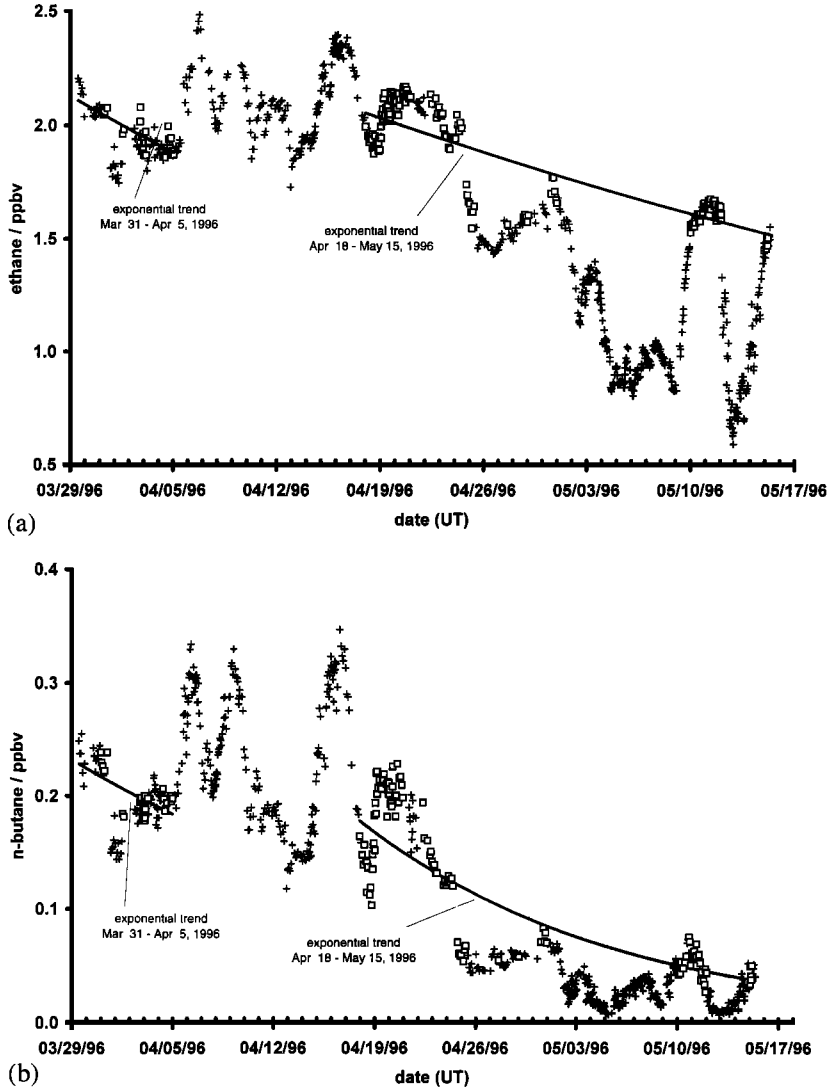

Figure 3. Examples of the estimate of $[alkane]_0$ from interpolation of the time series of (a) ethane and (b) n-butane mixing ratios found at ozone mixing ratios exceeding 30 ppbv. Fitting functions for data at ozone >30 ppbv are indicated in the figures. Crosses represent all data; squares represent alkane mixing ratios at ozone mixing ratios exceeding 30 ppbv within the interpolation limits.

4.2. Correlation Between Ozone and VOC

A summary of the correlation coefficients calculated for linear regressions of organic trace gas and ozone mixing ratios during depletion events is given in Table 4. The correlation coefficients for 2-methylbutane were calculated separately for the GC1 and GC2 data sets, since we observed a discrepancy between the results of the two analytical systems (see method comparison).

For the major ozone depletions, significant correlations to the ozone mixing ratio were observed for alkanes up to C_5, ethyne, tetrachloroethene, 2-propanone, and tribromomethane. All other monitored compounds did not show any significant correlation to ozone. During the minor depletion event, correlation coefficients were generally lower. Exceptions were found for butanes and 2-methylbutane. This was probably caused by the larger mixing ratios of these compounds during that period. Thus the concentrations were high enough to allow precise measurements. The weaker correlations between the mixing ratios of pentanes and ozone during the major ozone depletions were probably also caused by decreasing precision of the VOC measurements, since the mixing ratios were at the detection limit. Furthermore, since the mixing ratios are that low, the natural variability in the 2-methylbutane and n-pentane loading of the ozone depleted air masses could also mask a stronger correlation.

An anticorrelation between CO, dichloromethane, or bromomethane and ozone was found during the second major depletion in May. The slopes $d[VOC]/d[O_3]$ were small (CO: -0.18 pptv/ppbv, CH_2Cl_2: -0.06 pptv/ppbv, CH_3Br: -0.03 pptv/ppbv) but statistically significant. The change in these trace gases points toward air masses of different origin or history. This agrees with the general observation that the phenomenon of tropospheric ozone depletion is always connected with a change of air masses. However, the slopes $d[VOC]/d[O_3]$ were quite small, and the difference in VOC mixing ratio of the air masses was less than 8 ppbv (CO), 4 pptv (CH_2Cl_2), and 2 pptv (CH_3Br). This is still within the natural variability of these compounds for that season and year. Fur-

Table 3. Time Integrated Halogen Atom Concentrations and Meteorological Data for Different Ozone Depletion Episodes Calculated From the Changes in NMHC Mixing Ratios.

Episode in 1996	$\int [Cl \cdot]\,dt/10^9$ s cm^{-3}					$\int [Br \cdot]\,dt/10^{12}$ s cm^{-3}					Ozone, ppbv	Wind Speed, m/s	T, °C
	C_2H_6	C_3H_8	i-C_4H_{10}	n-C_4H_{10}	Mean	C_2H_6, C_2H_2	C_3H_8, C_2H_2	i-C_4H_{10}, C_2H_2	n-C_4H_{10}, C_2H_2	Mean			
April 1	2.5 ± 0.9	1.9 ± 1.5	1.7 ± 0.5	1.9 ± 0.3	2.0 ± 0.3	1.9 ± 1.3	2.2 ± 1.5	2.3 ± 1.4	2.2 ± 1.3	2.1 ± 0.2	19.6	5.4 (S)	−16.8
April 26	4.9 ± 1.8	4.7 ± 3.6	5.5 ± 1.5	4.4 ± 0.8	4.9 ± 0.5	0.2 ± 1.3	0.3 ± 2.0	−0.1 ± 1.3	0.4 ± 1.0	0.2 ± 0.2	28.9	3.3 (NNW)	−12.8
May 2	8.3 ± 2.1	5.9 ± 4.4	7.1 ± 2.3	5.1 ± 0.9	6.6 ± 1.4	1.0 ± 1.9	2.2 ± 2.6	1.7 ± 1.9	2.6 ± 1.6	1.9 ± 0.7	13.8	5.2 (SE)	−15.5
May 4	13.6 ± 2.8	13.5 ± 9.8	12.8 ± 3.4	*9.8 ± 2.4*	12.4 ± 1.8	5.8 ± 3.6	5.9 ± 5.8	6.2 ± 3.7	*7.7 ± 3.8*	6.4 ± 0.9	0.7	6.5 (NW)	−15.9
May 5	12.9 ± 2.7	10.1 ± 7.3	*10.6* ± 3.3	10.5 ± 1.8	11.0 ± 1.3	9.5 ± 4.8	10.9 ± 6.1	*10.7* ± 5.2	10.7 ± 5.0	10.5 ± 0.6	0.0	5.4 (WNW)	−18.6
May 6	12.0 ± 2.5	7.0 ± 5.1	2.4 ± 1.0	3.9 ± 0.8	6.3 ± 4.2	8.0 ± 4.2	10.5 ± 5.2	12.8 ± 5.4	12.1 ± 5.1	10.8 ± 2.1	0.4	1.1 (SE)	−11.4
May 8	9.7 ± 2.3	5.2 ± 3.9	1.2 ± 0.9	1.4 ± 0.6	4.4 ± 4.0	2.0 ± 2.1	4.3 ± 2.8	6.2 ± 2.6	6.1 ± 2.6	4.6 ± 2.0	6.0	0.2 (SE)	−11.7
May 13	14.0 ± 2.8	12.3 ± 8.9	10.5 ± 2.9	*8.3 ± 2.4*	11.3 ± 2.4	10.1 ± 5.1	10.9 ± 6.7	11.8 ± 5.5	*12.9 ± 5.7*	11.4 ± 1.2	1.0	6.5 (NNW)	−16.2

Italicized numbers were calculated from mixing ratios below the detection limit.

thermore, such behavior has not been observed for any other ozone depletion event encountered during the two ARCTOC field experiments. It is therefore not a general characteristic of ozone-depleted air masses.

A qualitative understanding of the substantially different VOC pattern of ozone-depleted air masses can be obtained from the analysis of the rates of reaction of VOC with halogen atoms and OH radicals. Table 2 lists the rate constants currently recommended by the National Institute of Standards and Technology (NIST) or Jet Propulsion Laboratory (JPL) publication 97-4 [*DeMore et al.*, 1997]. From the data, it becomes quite obvious that the ratio of the rate constants for reactions between VOC + Cl and VOC + OH, $k(Cl)/k(OH)$, is in the range of 50–600 for all compounds correlated with ozone during the depletion events (i.e., alkanes, ethyne, tetrachloroethene). For compounds which were not significantly correlated with the ozone mixing ratio that value is in the range of 0.2–20. In a previous study [*Ramacher et al.*, 1997] we were able to show that chlorine atom concentrations up to 10^5 cm^{-3} present for a time of 3 days would have significant impact on the alkane and ethyne concentrations in an air mass, whereas changes in CO, chloromethane, and benzene mixing ratios would be within the natural variability and the experimental error. Since the mixing ratios of several compounds were not changed significantly in ozone-depleted air masses, this strongly suggests that the tropospheric ozone depletions cannot be explained on a meteorological basis alone. Owing to the large number of monitored compounds, it becomes very likely that the presence of significant concentrations of free halogen atoms causes the observed phenomenon. This explanation fits qualitatively with the observed changes in VOC pattern. Solely, the anticorrelations between 2-propanone or tribromomethane and ozone mixing ratios cannot be explained. Tribromomethane is mainly of marine origin. Since ozone depletions were always linked to changes of air masses, this might suggest that ozone-depleted air masses had been in contact with open water. This theory was also favored by *Bottenheim* [1993] and *Hopper et al.* [1994]. The 2-propanone is different in its sources from the other monitored VOC (except ethanal), since it is not only directly emitted into the atmosphere but is also produced during the oxidation of hydrocarbons. Thus it seems reasonable that some of the hydrocarbons attacked by chlorine atoms during the depletion events form 2-propanone. This process might be able to explain the higher 2-propanone mixing ratios in ozone-depleted air masses. The most important 2-propanone precursor under arctic conditions is propane. Other hydrocarbons do not contribute significantly to the production of 2-propanone. It is only a minor product of the oxidation of 2-methylpropane. Higher hydrocarbons, which can form 2-propanone by fragmentation during the oxidation cycle, have not been observed at relevant mixing ratios during this study. The oxidation of propane by Cl proceeds via two possible pathways, with only (R1) being important for the formation of 2-propanone [*Tschuikow-Roux et al.*, 1985]:

$$\text{(R1)} \qquad Cl + C_3H_8 \rightarrow HCl + CH_3{-}CH{-}CH_3$$

$$k_{1,298K} = 6.1 \times 10^{-11}\ \text{cm}^3\ \text{s}^{-1}$$

$$\text{(R2)} \qquad Cl + C_3H_8 \rightarrow HCl + CH_2{-}CH_2{-}CH_3$$

$$k_{2,298K} = 5.5 \times 10^{-11}\ \text{cm}^3\ \text{s}^{-1}$$

Thus, for a change in propane mixing ratio from 340 to 50 pptv, as was observed during the last major depletion event, the

Table 4. Correlation Coefficients (r^2) for Linear Regression of VOC and Ozone Mixing Ratios During Ozone Depletion Episodes

Compound	Value of r^2			
	Whole Campaign	Minor Depletion	Major Depletion 1	Major Depletion 2
Ethane	0.825	0.834	0.953	0.954
Ethene	0.301	0.023	0.129	0.200
Ethyne	0.768	0.800	0.946	0.972
Propane	0.599	0.929	0.861	0.940
Propene	...	...	...	
2-methylpropane	0.408	0.767	0.442	0.844
n-butane	0.478	0.867	0.638	0.773
2-methylbutane	0.367/0.458	0.772/...	0.257/0.290	0.505/0.537
n-pentane	0.287	0.417	0.428	0.617
n-hexane	0.003	0.164	...	...
n-heptane	0.006	0.088	...	...
Benzene	0.258	0.412 (−)	0.114 (−)	0.149 (−)
Toluene	0.085 (−)	0.054 (−)	...	...
Ethylbenzene	0.062		0.000 (−)	...
Dimethylbenzenes	...	...	...	...
Ethanal	0.010	0.060	0.006 (−)	0.368
2-propanone	0.340 (−)	0.672 (−)	0.719 (−)	0.792 (−)
Chloromethane	0.019 (−)	0.338	0.026	0.255
Dichloromethane	0.109	0.027	0.252 (−)	0.671 (−)
Trichloromethane	0.019	0.035	0.046	0.352
Tetrachloromethane	0.466	0.000	0.039	0.450
1,1,1-trichloroethane	0.028 (−)	0.312 (−)	0.007	0.097
Tetrachloroethene	0.856	0.726	0.937	0.956
Bromomethane	0.459 (−)	0.006 (−)	0.356 (−)	0.619 (−)
Dibromomethane	0.025	0.078 (−)	0.037 (−)	0.005
Tribromomethane	0.011 (−)	0.671 (−)	0.718 (−)	0.536 (−)
Iodomethane	0.001	0.000 (−)	0.021 (−)	0.497
CO	0.113	0.000	0.354 (−)	0.633 (−)

Negative correlations are marked (−); VOC mixing ratios have not been corrected for the seasonal trend. For 2-methylbutane the correlation to ozone was calculated separately for the two data sets. GC1 data are given first, and GC2 data second. Minor depletion ranges from March 31, 1996, 0000 to April 2, 1996, 2400; major depletion 1 ranges from April 30, 1996, 0000 to May 10, 1996, 2400; and major depletion 2 ranges from May 11, 1996, 0000 to May 15, 1996, 1300.

2-propanone formation amounts to 150 pptv at maximum, ignoring the 2-propanone destruction by chlorine atoms, which is about 20 times slower. The observed 2-propanone increase during that event was of the order of 250 pptv, which is somewhat higher than the estimate made above. Furthermore, it should be noted that the 2-propanone mixing ratio was calculated from a mean carbon response. There have been several publications on the sensitivity of FIDs toward organic compounds [e.g., *Ackman*, 1964; *Dietz*, 1967; *Ettre*, 1962; *Scanlon and Willis*, 1985; *Sternberg et al.*, 1962]. These investigations showed that the FID sensitivity for 2-propanone is about 50–70% of that for propane, depending on the burning conditions in the detector. Correcting the calibration given here with the sensitivity found in these studies would lead to an increase of the 2-propanone mixing ratios up to a factor of 2. Hence the difference between the measurements and the estimate of 2-propanone production becomes even larger. Presently, there is no satisfactory explanation for this anticorrelation, which has also been observed by *Yokouchi et al.* [1994].

4.3. Correlations Among Hydrocarbon Mixing Ratios

Another way to look at the changes in the VOC pattern during ozone depletions is to plot the mixing ratios of selected VOC against each other. To detect the impact of chlorine atom chemistry on a ratio of trace gas concentrations during ozone depletion events, the influence of mixing and photochemical aging by reaction with OH radicals must be reduced to a minimum. This can be achieved by selecting compounds with similar lifetimes toward reaction with OH radicals and very different lifetimes toward reaction with chlorine atoms. In this case the influence of air mass mixing and dilution will become negligible if the initial VOC pattern of the air masses is not too different, i.e., the source distribution of the compounds is similar. (For details on changes of NMHC pattern during mixing and transport, see *McKeen and Liu* [1993].) In the case of the spring arctic troposphere this approximation seems quite reasonable. First, the mixing ratios of a large number of organic trace gases like methane [*Ramacher*, 1997], peroxyacetylnitrate (PAN) [*Buskühl*, 1996], and most halocarbons do not change significantly in ozone-depleted air masses. Second, when comparing measurements from different stations throughout the arctic, the observed mixing ratios of longer lived VOC (C_2–C_4 alkanes, ethyne, and benzene) appear to be rather similar [*Jobson et al.*, 1994; *Ramacher*, 1997].

Given the reactivity data in Table 2, tetrachloroethene/dichloromethane, propane/benzene, 2-methylpropane/n-butane, n-hexane/toluene, or n-heptane/toluene would be suitable pairs for this kind of analysis. Owing to the low mixing ratios of compounds with more than five carbon atoms, the errors of such an evaluation become too large to be meaningful. Additionally, the influence of local sources like fossil fuel combustion or evaporation losses was found to be much more pronounced for these compounds. Therefore we investigated

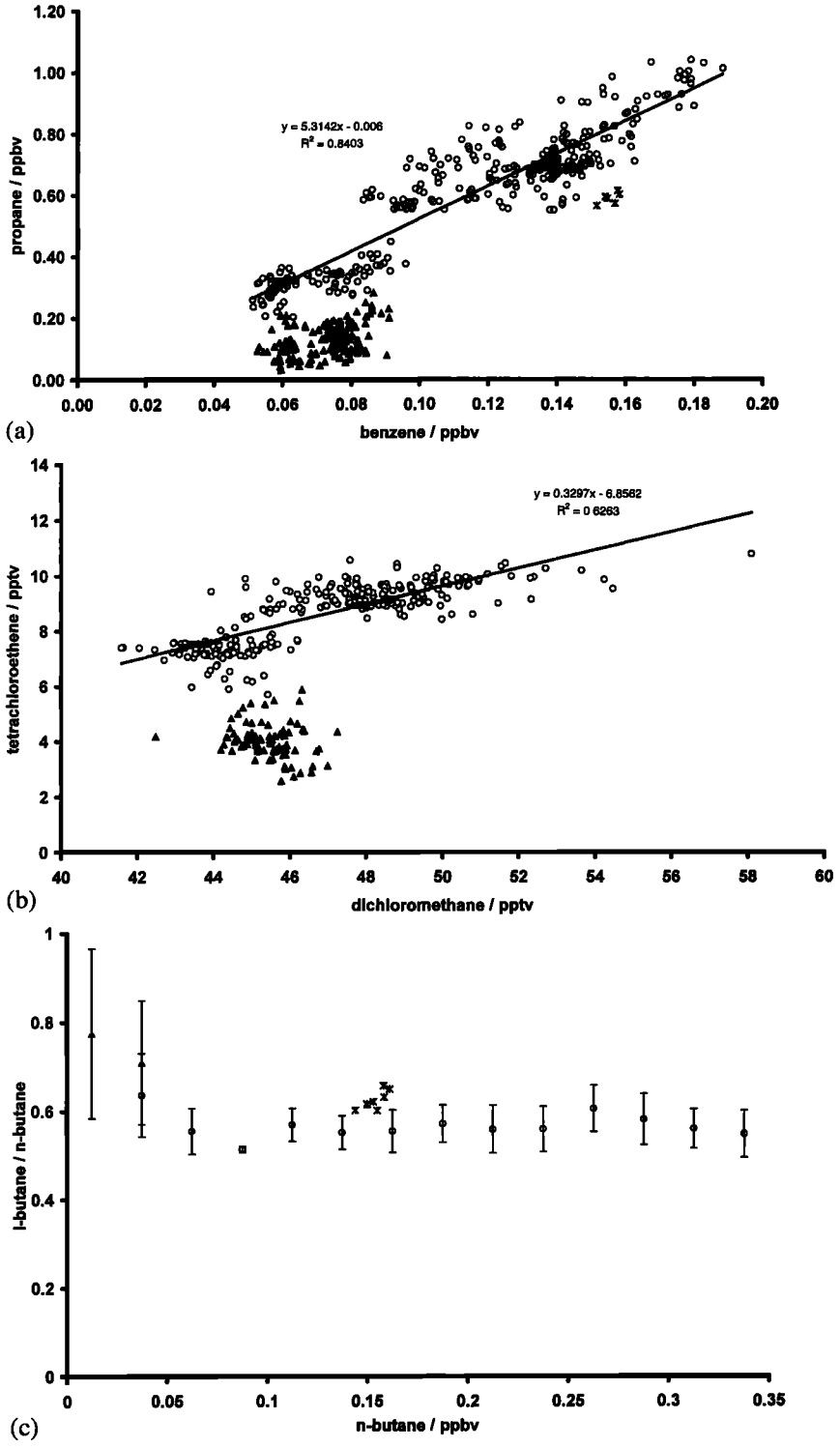

Figure 4. VOC with similar lifetimes toward removal by OH radicals plotted as pairs: (a) propane versus benzene, (b) tetrachloroethene versus dichloromethane, and (c) 2-methylpropane/n-butane ratio versus n-butane. Circles are background data (O_3 > 30 ppbv); asterisks, minor depletion period (March 31 to April 2, O_3 < 20 ppbv); and triangles, major depletion period (April 30 to May 15, O_3 < 20 ppbv; Figure 4c shows mean value ± standard deviation for 0.025 ppbv intervals of n-butane mixing ratio). Regression lines in Figures 4a and 4b are fitted to the nondepletion data (O_3 > 30 ppbv).

only the propane/benzene, tetrachloroethene/dichloromethane, and 2-methylpropane/n-butane ratios (Figures 4a–4c). To smooth out the scattering, the latter pair is plotted as the mean 2-methylpropane/n-butane ratio for 25 pptv intervals of n-butane. In the cases of tetrachloroethene/dichloromethane and propane/benzene the data recorded during the major ozone events at ozone mixing ratios less than 25 ppbv differs significantly from the overall trend recorded at ozone mixing ratios

exceeding 30 ppbv. For the minor ozone depletion period this difference was less pronounced (since the halocarbon measurements started on April 6, there are no data shown in Figure 4b). The scatter of the ratio of 2-methylpropane and n-butane was quite large during the major depletion periods (Figure 4c). This was probably due to the increasing experimental errors, since the butane mixing ratios already approached the detection limit. However, the mean values still differ slightly from the data recorded at "normal" ozone levels. This holds also true for the minor depletion period.

The difference in the mixing ratios in ozone-depleted air masses to those at normal ozone concentrations was smallest for 2-methylpropane/n-butane. This can be explained by a different sensitivity of these pairs toward the presence of free chlorine radicals. The ratio of the rate constants is about 330 for $k_{\text{tetrachloroethene,Cl}}/k_{\text{dichloromethane,Cl}}$, about 16,500 for $k_{\text{propane,Cl}}/k_{\text{benzene,Cl}}$, and only 1.3 for $k_{\text{2-methylpropane,Cl}}/k_{\text{n-butane,Cl}}$.

A more detailed analysis of the propane/benzene data obtained at "normal" ozone levels showed that this data set can be further separated into subsets with different propane/benzene ratios. For benzene mixing ratios between 60 and 120 pptv, substantial deviations of the propane/benzene ratio from the regression line were found (Figure 4a). A first subset with benzene mixing ratios between 60 and 100 pptv (all data collected between April 24 and May 2) generally had a lower propane/benzene ratio, whereas a second subset (benzene mixing ratios between 80 and 120 pptv, all data collected between April 14 and 24) always had higher propane/benzene ratios than the average. The tetrachloroethene/dichloromethane ratio behaves very similarly during these two periods of time but will not be discussed in detail here. Three-day back trajectory calculations performed by the Danish Meteorological Institute indicated that between April 14 and 19 the air masses were advected to the measurement site from a northeasterly to easterly direction and originated from Asia (Figure 5a). Between April 20 and 22 the local wind speed decreased to less than 1 m/s. Back trajectories show that during this period the air masses were moving in close vicinity to the measurement site within the last 3 days (Figure 5b). Starting on April 23, the local wind speed increased considerably, and the trajectories shifted from the North Atlantic (April 23) via Iceland (April 24) to northern Greenland (April 25, Figure 5c). Until April 28, the air masses originated from northeastern Greenland. Instead of being advected directly to Ny Ålesund from the west, they reached the measurement site from the east after passing over the southern tip of Svalbard. Between April 29 and May 2, the air masses were still advected from the east but originated from Novaja Zemlja and, later, from closer to the pole (Figure 5d). On May 3 the local wind direction shifted to northwest, and ozone-depleted air was advected to Ny Ålesund instantaneously.

We believe that the changes in the propane/benzene ratio between April 14 and May 2 are due to the different origin of the air masses. Both compounds have rather similar lifetimes toward reaction with OH radicals, but their sources are quite different. The main sources for benzene are the evaporation and burning of gasoline, whereas propane sources are closely linked to sources of natural gas [*Warneck*, 1988]. Thus it seems reasonable that during the period between April 14 and 24 the propane/benzene ratio reached its maximum, since the air masses passed over northern Europe or northern Asia, where propane sources are more dominant compared to the benzene sources.

The lower propane/benzene ratios observed between April 25 and May 2 are correlated with a decrease in ozone mixing ratio (about 15 ppbv lower than during the April 14–24 period). The trajectories indicate that the air masses came quite close to the pole before reaching Ny Ålesund. Therefore it seems possible that they were depleted in ozone but were mixed with undepleted air afterward. In this case, the propane/benzene ratio would be lowered compared to background air. To some extent this is confirmed by the bromine oxide measurements [*Martinez-Walter et al.*, 1997; *Ackermann et al.*, 1997]. They observed increased BrO concentrations compared to the background during that period, which strongly indicates that there has been some influence by free halogen atoms.

Although the trajectories on May 2 and 3 (Figures 5d and 5e) were almost identical, a significant ozone depletion was observed when the local wind direction shifted from southeast to northwest on May 3. This is most probably caused by the local topography. Air masses coming in from the northwestern sector pass over the Arctic Ocean, whereas air masses coming in from the east have to pass the mountain chains with heights of 1200 m and more. In that case, mixing with ozone rich air from the free troposphere is likely, and ozone depletions are rarely observed [*Hopper et al.*, 1994; *Solberg et al.*, 1996].

This discussion shows the problems of this kind of analysis. One has to compare compounds having similar lifetimes with OH radicals and similar source distributions. This is the case for 2-methylpropane/n-butane. However, the reaction rates of these two compounds with Cl do not differ that much, so that the change in the 2-methylpropane/n-butane ratio during ozone depletions is not very large. Additionally, the mixing ratios of these compounds were close to the detection limit, which resulted in a larger error. For the pairs propane/benzene and tetrachloroethene/dichloromethane it is just the other way around. Here the rate constants with Cl are very different, but the source distributions might be different too (e.g., for benzene, fossil fuel leakage, combustion; for propane, natural gas).

Nevertheless, we were able to examine three pairs of compounds and the observed changes in the hydrocarbon pattern are consistent with chlorine atom processing.

4.4. Time Integrated Halogen Atom Concentrations

The results presented in Table 3 have shown that the integrated chlorine atom concentrations calculated on the basis of changes in alkane mixing ratios are in good agreement for most of the campaign. However, this was not the case during the period between May 5 and 9. This becomes obvious from Figure 6, which shows the time series of the time integrated chlorine atom concentration between April 28 and May 12, calculated from the change in four different alkanes, ethane, propane, 2-methylpropane, and n-butane. The time series were calculated by solving (1) for each data point. Between April 28 and May 5, the difference between the integrated chlorine atom concentrations was smaller than 2.5×10^9 s cm^{-3} and obviously statistically not significant. The same holds true for the period between May 9 and 12. However, between May 5 and 9, the integrated chlorine atom concentrations calculated from the four different alkanes differed significantly. The calculated time integrated chlorine atom concentration based on the changes in n-butane is always smaller than the chlorine atom concentration based on propane or that based on ethane, which always gave the largest values. There are three possible explanations for this observation.

A first cause could be the use of inadequate rate constants.

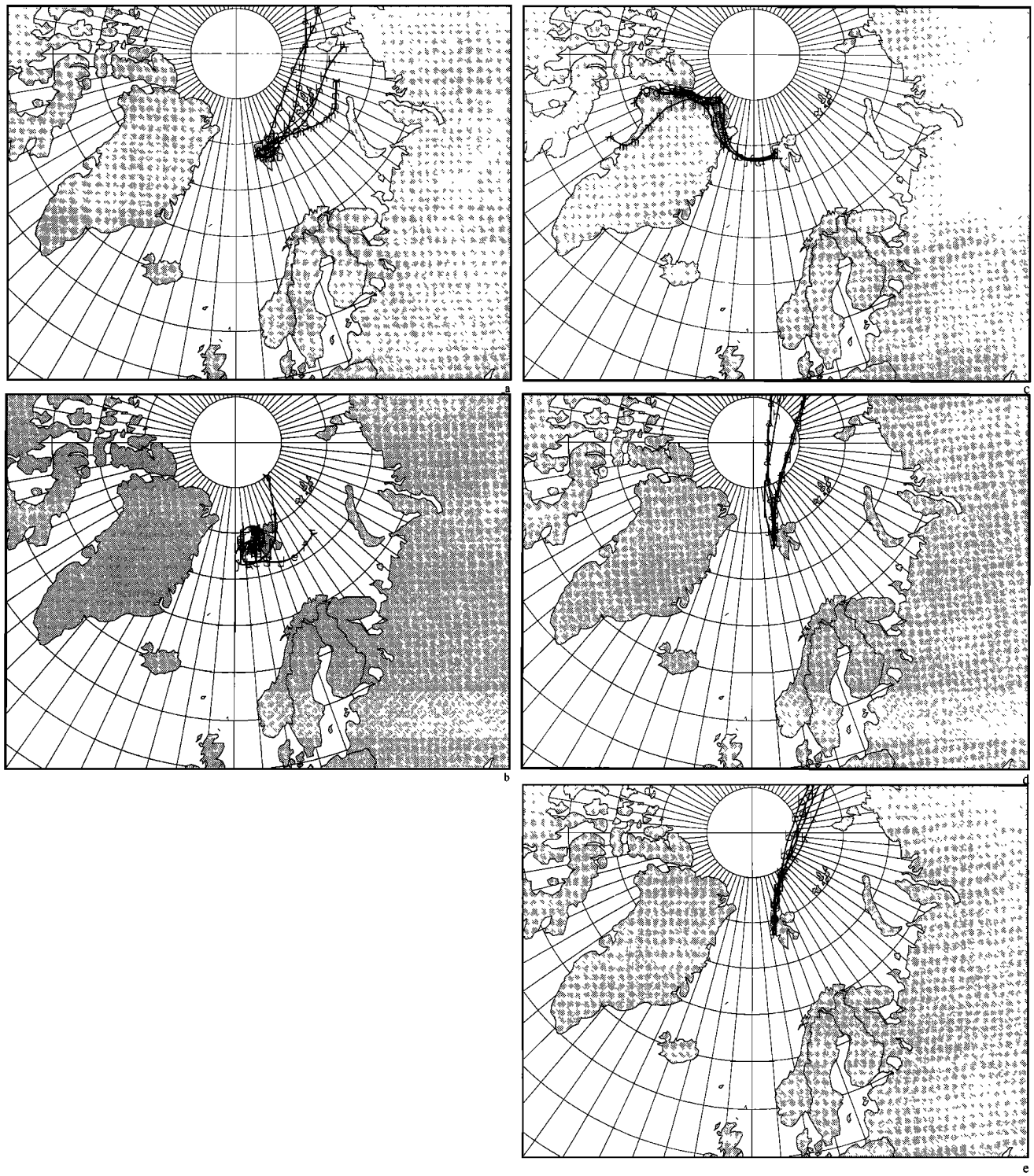

Figure 5. Three-day back trajectories for Ny Ålesund calculated by the Danish Meteorological Institute, Copenhagen, for (a) April 15, 1996, 1800; (b) April 21, 1996, 1800; (c) April 25, 1996, 0600; (d) May 2, 1996, 0600; and (e) May 3, 1996, 0600. Letters mark 6 hour time intervals and indicate the height above sea level in steps of 250 m (a, 0–250 m; b, 250–500 m, etc.).

This should affect the complete time series and result in a constant offset between the integrated chlorine atom concentrations based on the three alkane concentrations. However, at normal ozone mixing ratios or during minor depletions the natural variability of the alkane pattern could possibly mask this effect because of the small chlorine atom concentrations, so that their effect is observed only at lower ozone mixing ratios. The rate constants used in this study were taken from different publications; thus using data from studies of relative rate constants should result in better agreement between the

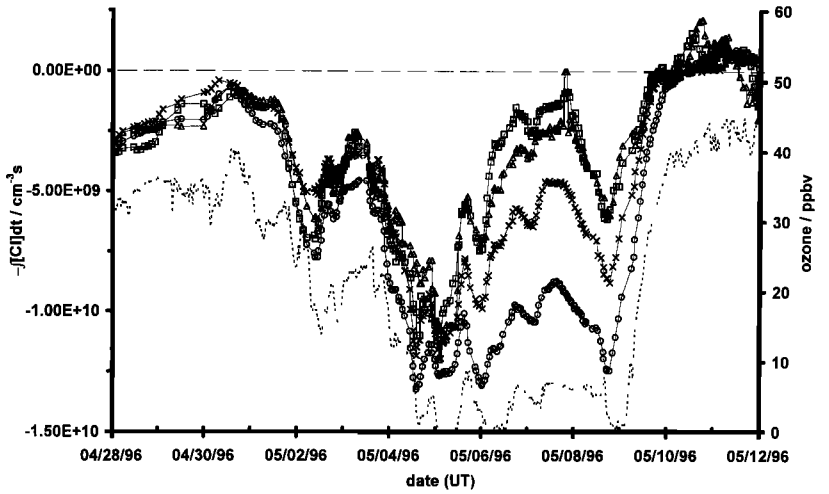

Figure 6. Time integrated chlorine atom concentrations calculated from changes in different alkanes for the period April 28 to May 12, 1996 (running mean of five data points). Symbols represent calculation based on ethane (circles), propane (crosses), 2-methylpropane (squares), and n-butane (triangles). Dashed line represents ozone. Negative integrated chlorine atom concentrations are plotted to demonstrate correlation with ozone.

different sets of integrated chlorine atom concentrations. Using either the data of *Hooshiyar and Niki* [1995], *Wallington et al.* [1988], or *Atkinson and Aschmann* [1985] did not alter the results significantly. Furthermore, this argument is weakened by the rather small differences of the integrated chlorine atom concentrations prior to May 5, when the ozone mixing ratio was also very low. Hence the differences in the integrated chlorine atom concentrations cannot be explained satisfactorily by the use of inadequate rate constants.

As a second explanation, one could argue that the air masses examined between May 5 and 9 were special in some respect. One possibility would be that the estimate of the initial alkane concentrations was incorrect. In order to obtain a consistent result (i.e., the mean integrated Cl atom concentration calculated from the four alkanes) for May 7, the initial ethane concentration would have to be lowered from 1655 to 1272 pptv, and the initial propane, 2-methylpropane, and n-butane mixing ratios would have to be raised from 303 to 351, from 34 to 51, and from 58 to 91 pptv, respectively. All values are far beyond the errors in the estimates of the initial alkane concentrations (<10%; see results). A third possibility would be that the meteorological situation for the period of May 5–9 changed and enhanced mixing with other air masses. Temperature, wind speed, and wind direction during selected depletion periods are listed in Table 3. In general, substantial ozone depletions were observed at low air temperature and wind speeds larger than 5 m/s from the northwest. This is in agreement with observations of *Solberg et al.* [1996], who analyzed the meteorological situations and trajectories of ozone-depleted air masses arriving at Ny Ålesund. They found that low ozone periods were only observed if the trajectories lay in the northern to western sector. The local temperature in ozone-depleted air masses was well correlated to the ozone mixing ratio and about 4°C lower than the average. Between May 5 and 9, the air temperature was relatively high (−10 to −11°C), and the wind speed generally lower than 1.5 m/s. Additionally, frequent changes between easterly and westerly wind were observed. Figure 7 presents a trajectory calculation by the Danish Meteorological Institute for Ny Ålesund, May 8, 1996, 0600 UT. The trajectories indicate that the air masses arriving at Ny Ålesund during this period were circulating around Svalbard. Altogether, the data presented here show that the meteorological situation during the May 5–9 period was quite different from the situation during typical ozone depletion events. This suggests that the ozone-depleted air was mixed with other air masses. This can be confirmed by data from ozone soundings [*Koenig-Langlo and Marx*, 1997] made on May 4, 6, and 8 (Figure 8). On May 4 the partial ozone pressure varied between 1.2 and 1.5 mPa at ground level and was almost constant at 1.2 mPa from 350 to 1300 m. Above that was free tropospheric air with an ozone pressure of the order of 3.5 mPa.

On May 6 the picture had changed significantly. The ozone depletion at ground level increased. Up to a height of 500 m the partial ozone pressure was constant at 0.2 mPa. Above that

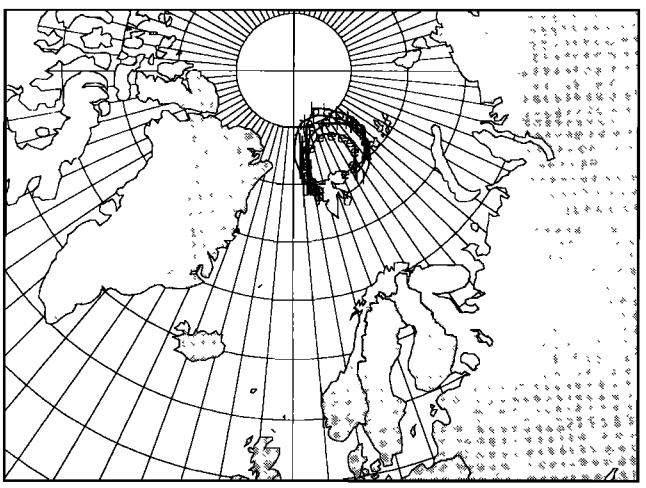

Figure 7. Trajectory calculation by Danish Meteorological Institute for Ny Ålesund, May 8, 1996, 0600 UT. Letters mark 6 hour time intervals and indicate the height above sea level in steps of 250 m, (a, 0–250 m; b, 250–500 m, etc.).

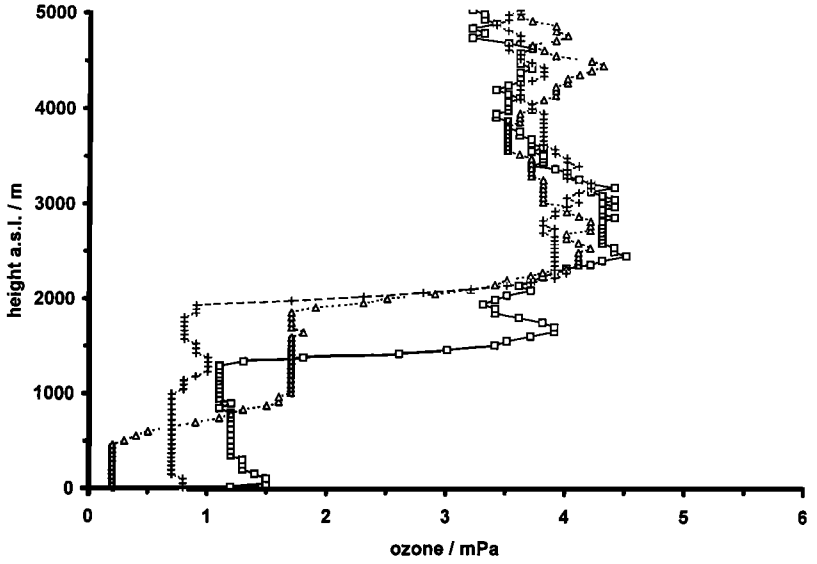

Figure 8. Height profile of the partial ozone pressure measured by balloon-borne ozone soundings. Data taken from *Koenig-Langlo and Marx* [1997]. Squares, May 4, 1996, 1135 UT; triangles, May 6, 1996, 1118 UT; crosses, May 8, 1996, 1113 UT.

lower layer of air, the ozone partial pressure increased almost linearly with height to 1.7 mPa at 900 m above sea level. Between 900 and 1900 m a second well-mixed layer of air was observed that had also lost some ozone (partial pressure 1.7 mPa). Above this layer, free tropospheric air was sampled. The data for May 8 suggest that the two separate air masses seen on May 6 had mixed because the partial ozone pressure was now at an intermediate level (~0.8 mPa) up to a height of 2000 m. Above this, the sonde entered the free troposphere. This explains why we obtained different integrated chlorine atom concentrations depending on the compound chosen for the calculation. Both air masses had already undergone an ozone depletion but to a different extent. This means that their age in terms of an integrated chlorine concentration was different. Due to the different reaction rates between chlorine atoms and the selected alkanes, the integrated chlorine atom concentrations will depend on the alkane as soon as the two air masses are mixed.

As an example, consider initial mixing ratios of ethane, propane, 2-methylpropane, n-butane, tetrachloroethene, and benzene of 2000, 1000, 100, 200, 20, and 200 pptv, respectively, in two air masses of the same volume.

With integrated Cl concentrations of 10^9 $cm^{-3}s$ in air mass 1 and 10^{10} $cm^{-3}s$ in air mass 2, the mixing ratios given in Table 5 will result from the mixing of both air masses. It can easily be seen that the integrated Cl concentrations calculated for the air mass mix are compound dependent. They decrease with increasing reactivity of the compounds toward Cl atoms, which is in agreement with the observations presented here. A detailed description of the effects of mixing on hydrocarbon mixing ratios has been published by *McKeen and Liu* [1993].

Since the integrated bromine atom concentrations depend on the integrated chlorine atom concentration (2) the remaining question is, Which compound should be used to calculate the time integrated chlorine atom concentration? In our opinion, this question cannot be answered with the available data. One piece of information can be obtained from the correlation between ozone and the light alkanes for the period between May 5 and 9. During low ozone periods a good correlation between ozone and light hydrocarbons has generally been observed in the past [*Jobson et al.*, 1994; *Solberg et al.*, 1996; *Ramacher et al.*, 1997]. For a linear regression to our data the correlation coefficients (r^2) were found to be 0.77 (ethane), 0.79 (ethyne), 0.42 (propane), 0.06 (2-methylpropane), and 0.16 (n-butane). This suggests that the butanes and propane mixing ratios were significantly affected by mixing processes discussed above. The correlation between ozone and ethane is also lowered compared to the numbers given in Table 4, but it

Table 5. Example Showing That Compound Dependent Integrated Cl Concentrations Will be Calculated for an Air Mass Made Up From a Mix of Two Air Masses Having Different Ages in Terms of Integrated Chlorine Concentrations

Compound	k_{Cl+VOC}, 10^{-14} cm^3 s^{-1}	Air Mass 1, pptv	Air Mass 2, pptv	Mix of Air Mass 1 and 2, pptv	Mix of Air Mass 1 and 2,* $\int$ [Cl] $dt/10^9$ cm^{-3} s
Ethane	5,370	1895	1169	1532	4.96
Propane	14,100	868	244	556	4.16
i-butane	15,100	86	22	54	4.08
n-butane	19,700	164	28	96	3.72
C_2Cl_4	4,610	19	13	16	5.04
Benzene	0.85	200	200	200	5.50

*The integrated Cl concentrations have been calculated from the mixing ratios in the mixed air mass (previous column) and the initial mixing ratios given in the text.

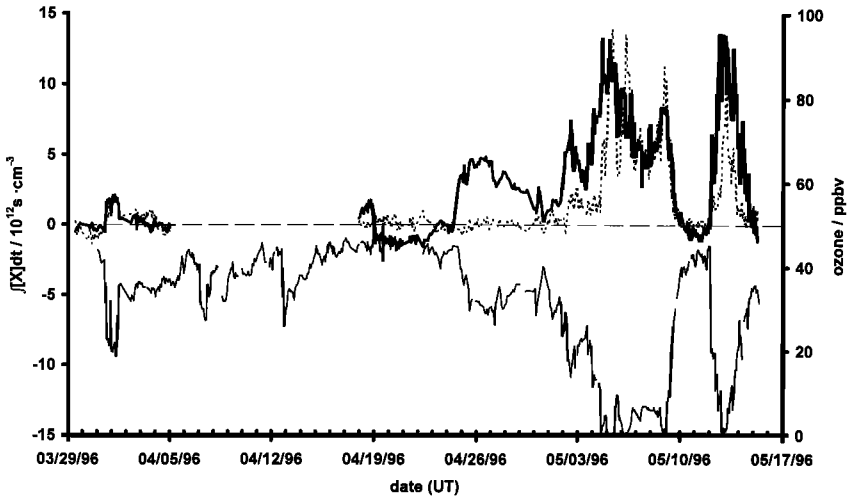

Figure 9. Time integrated chlorine and bromine atom concentrations calculated from changes in hydrocarbon pattern. Bold line, $\int$ [Cl] $dt \times 1000$; dotted line, $\int$ [Br] dt; thin line, ozone.

is certainly the compound which was least affected. However, there is a lack of information on other important trace gases such as NO_x. Some of these strongly affect the net destruction of ozone by halogen atoms but are not significant for the removal of VOC by halogen atoms (see below). Therefore we decided to use the mean integrated chlorine atom concentration calculated from the change in the light alkanes for the following analyses.

4.5. Time Series of Time Integrated Halogen Atom Concentrations

Figure 9 shows time series of the integrated halogen atom concentrations. They were calculated by solving (1) and (2) for each hydrocarbon data point within the time periods for the extrapolation given in Figures 3a and 3b. The time integrated chlorine atom concentration is given as the mean of the integrated chlorine atom concentrations calculated from individual alkanes. At background ozone mixing ratios ($O_3 > 30$ ppbv) our calculations yielded no significant integrated halogen atom concentrations, which resulted from the definition of the initial concentrations $[\text{alkane}]_0$ and $[\text{ethyne}]_0$. For these conditions the mean integrated chlorine and bromine atom concentrations were $5 \pm 14 \times 10^8$ and $9 \pm 42 \times 10^{10}$ s cm^{-3}, respectively. During ozone depletion events these values increase by more than a factor of 10. A closer analysis reveals that during each ozone depletion event the integrated chlorine atom concentration increases earlier than the integrated bromine atom concentration and remains at high levels for a longer period of time. The bromine atom concentration starts to increase when ozone mixing ratios are below 15–20 ppbv and reaches very high levels for ozone <5 ppbv. This is most obvious for the period of April 24–30, where in contrast to the integrated bromine atom concentration, the time integrated chlorine atom concentration is significantly different from zero. Our current understanding is that this points toward the different impacts of VOC and ozone on the halogen atom lifetimes.

The lifetimes of bromine atoms is about 1.4 s with respect to reaction with 40 ppbv ozone, 60 s with respect to 200 pptv ethanal, and 800 s with respect to 300 pptv ethyne. Thus, initially, the Br lifetime is determined by reaction with ozone. Since the recycling of BrO formed in that reaction is the rate determining step, the bromine atom concentration will be low. With decreasing ozone, the bromine atom concentration will increase, and the reaction with ethyne becomes more important. The resulting change in the ethyne concentration will then exceed the natural variability, the experimental errors, and the ethyne destruction by chlorine atoms. The reaction times for chlorine atoms with 1.86 ppmv methane, 1.6 ppbv ethane, 350 pptv propane, 300 pptv ethyne, 60 pptv n-butane, and 40 ppbv ozone are 0.5, 0.4, 0.7, 1.5, 2.9, and 0.1 s, respectively. Hence the chlorine atom concentration is as sensitive to alkanes as to ozone. Since the chlorine atom lifetime is not strongly dependent on the ozone concentration, the chlorine atom concentration should be almost constant during the depletion event (assuming constant primary production and recycling of Cl atoms).

This hypothesis is supported by the BrO measurements [*Martinez-Walter et al.*, 1997; *Ackermann et al.*, 1997], which yielded significant concentrations of BrO for the April 24–30 period (up to 1.8×10^8 cm^{-3}). However, bromine atoms could not be detected by monitoring the ethyne mixing ratio in that air mass because the ozone concentrations were high. Model calculations support this argumentation. They indicate that the concentration of free bromine atoms increases dramatically for ozone mixing ratios below 10 ppbv, whereas the chlorine atom concentration is almost independent of the ozone concentration [*Borken*, 1996].

Another possibility for the observed difference in the time evolution of the integrated halogen atom concentrations may be the source of halogen atoms. So far, it is generally assumed that chlorine and bromine atoms are injected into an air mass at the same time by a similar or a combined mechanism. This, of course, needs to be investigated, since chlorine and bromine sources could act separately, and these compounds could come into play independently, i.e., there could be significant amounts of chlorine without bromine atoms, and vice versa.

4.6. Estimate of the Ozone Change During Ozone Depletion Periods

In previous publications [*Jobson et al.*, 1994; *Ramacher et al.*, 1997] the ozone change caused by the presence of chlorine and bromine atoms in an ozone-depleted air mass was estimated

under the assumption that each reaction between halogen atoms and ozone results in a net ozone loss ((3), (R3)):

$$\left(\frac{[O_3]_X}{[O_3]_0}\right) = \exp\left(-k_{O_3,Cl}\int [Cl]\,dt - k_{O_3,Br}\int [Br]\,dt\right) \quad (3)$$

where $[O_3]_{X/0}$ is the concentration of ozone during depletion (subscript X) and in background air (subscript 0), $k_{O_3,X}$ is the rate constant for the reaction between ozone and X (X = Cl, Br), and $[Y]$ is the trace gas concentration (Y = Br, Cl, O_3).

This is not the case, since there are reaction cycles, which could enhance the destruction of ozone (e.g., by additional RO_2 radicals formed due to halogen-atom-induced VOC removal, (R4) and (R5)) or slow down the ozone destruction (e.g., by ozone formation through NO_2 photolysis, NO_2 formation by reaction of NO with BrO). In this respect, the following reactions are potentially important:

(R3) $\quad Br + O_3 \rightarrow BrO + O_2$

(R4a)

$$X + R^1 - H \rightarrow R^1O_2 + HX \qquad (X = Br, Cl; R^1 = \text{alkane, aldehyde})$$

(R4b)

$$X + R^2 \rightarrow \text{halogenated organics} \qquad (X = Br, Cl; R^2 = \text{alkene, alkyne})$$

(R5) $\quad RO_2 + O_3 \rightarrow RO + 2O_2$

(R6) $\quad NO + XO \rightarrow NO_2 + X$

(R7) $\quad NO + O_3 \rightarrow NO_2 + O_2$

(R8) $\quad NO_2 + h\nu + O_2 \rightarrow NO + O_3$

(R9) $\quad NO_2 + XO \rightarrow XONO_2$

(R10) $\quad BrO + h\nu + O_2 \rightarrow Br + O_3$

(R11) $\quad Cl + O_3 \rightarrow ClO + O_2$

(R12) $\quad ClO + h\nu + O_2 \rightarrow Cl + O_3$

(R13) $\quad 2BrO \rightarrow 2Br + O_2$

(R14a) $\quad ClO + BrO \rightarrow OClO + Br$

(≈50% yield)

(R14b) $\quad ClO + BrO \rightarrow Cl + Br + O_2$

(≈50% yield)

(R15) $\quad OClO + h\nu + O_2 \rightarrow ClO + O_3$

Considering the slow rate constant of (R5), the effect of additional RO_2 radicals formed by (R4a) can be neglected because measurements by *Arnold et al.* [1997] showed that the RO_2 concentration during depletion events reaches maxima of just 5 pptv. At an ozone mixing ratio of 40 ppbv and an RO_2 mixing ratio of 5 pptv, only about 1 ppbv of ozone would be destroyed per day.

The significance of the reactions involving NO_x is difficult to address, since NO_x was not measured during the ARCTOC 96 campaign. Previous measurements [*Beine et al.*, 1997] and, especially, model calculations [e.g., *Sander et al.*, 1997] indicate that the NO_x concentration should be very low during major ozone depletion periods. This denitrification is explained by the formation of chlorine and bromine nitrate (R9), which are stable reservoir compounds that can be scavenged by aerosol particles. Assuming this is correct, (R6)–(R8) can also be neglected, leaving the "do nothing" cycles of (R3) and (R10)–(R12), as well as the more complex reactions (R14a) and (R15).

In order to investigate this in more detail, we used the model calculation performed by *Borken* [1996]. It is a box model considering a total of 40 compounds and 84 reactions including gas phase chemistry of some hydrocarbons, HO_x, NO_x, halogen compounds, and photolysis. Heterogeneous recycling of halogen compounds is also added but is a simplification of the models by *Sander et al.* [1997] and *Vogt et al.* [1996]. Explicitly, the following reactions are included:

(R16) $\quad HBr\,(g) \rightarrow HBr\,(aq)$

(R17a) $\quad HOBr\,(g) \rightarrow HOBr\,(aq)$

(R17b) $\quad HOBr\,(aq) \rightarrow HOBr\,(g)$

(R18) $\quad BrONO_2\,(g) \rightarrow HOBr\,(aq) + HNO_3$

(R19) $\quad HBr\,(aq) + HOBr\,(aq) \rightarrow Br_2$

The transfer coefficients of (R16)–(R18) were scaled to the work of *Vogt et al.* [1996], incorporating aerosol distribution, diffusion, and accommodation under the assumption that this process is rate determining:

(R20) $\quad HCl\,(g) \rightarrow HCl\,(aq)$

(R21) $\quad HOCl\,(g) \rightarrow HOCl\,(aq)$

(R22) $\quad ClONO_2\,(g) \rightarrow HOCl\,(aq) + HNO_3$

(R23) $\quad HCl\,(aq) + HOCl\,(aq) \rightarrow Cl_2$

(R24) $\quad HOBr\,(aq) + HCl\,(aq) \rightarrow BrCl$

Again the phase transfer is assumed to be rate determining with the transfer coefficients of (R20)–(R22) scaled relative to the Br chemistry according to the ratios given by *Sander et al.* [1997].

The model considers no loss of halogen atoms to halogenated organics by addition reactions of halogen atoms to ethene or ethyne (R4b); all reactions between halogen atoms and VOC lead to the formation of *HX* (R4a). HONO and the production of OH by HONO photolysis have also not been considered in the model for two reasons. First, benzene mixing ratios do not change significantly during the depletion events. If significant amounts of OH radicals (produced by HONO photolysis) had been present, the benzene mixing ratio should have decreased during the events. Second, modeling studies [*Sander et al.*, 1997; *Vogt et al.*, 1996] have shown that the NO_x concentration in ozone-depleted air is very low because all NO_x is transformed to nitrates and transferred to the aerosol. Consequently, there should be no significant gas phase production of HONO via OH + NO.

Li [1994] reported a HONO mixing ratio of 10 pptv for an ozone depletion event observed in Alert on April 5, 1992. Together with the photolysis frequency for HONO, they came up with an OH concentration of 3×10^5 cm^{-3}. However, this seems not to be the general situation. During a second ozone

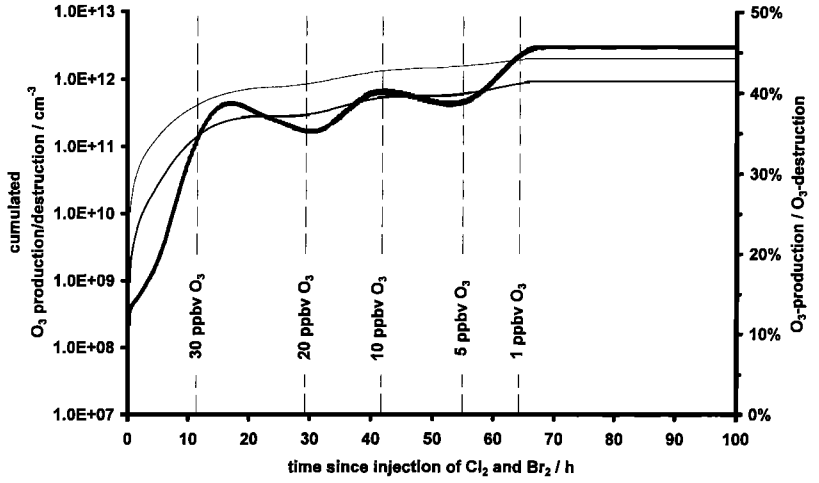

Figure 10. Results of a box model calculation [*Borken*, 1996]. Cumulated ozone production (BrO + $h\nu \rightarrow$ Br + O_3), destruction (Br + $O_3 \rightarrow$ BrO) and their ratio since the injection of the halogen molecules into the box. Vertical lines mark the time at which the ozone mixing ratio in the box has the given value. Thin line, ozone destruction (R7); medium line, ozone production (R8); thick line, ratio of cumulated ozone production and cumulated ozone destruction.

depletion event on April 9–10, 1992, the same author reported HONO concentrations below the detection limit.

Halogen atom chemistry is started after 72 hours by a single injection of 50 pptv of Cl_2 and 50 pptv of Br_2. These amounts were chosen to yield BrO and ClO concentrations similar to those measured by *Tuckermann et al.* [1997] during the ARCTOC 95 and 96 experiments. Ozone is then depleted within 65 hours from an initial mixing ratio of 40 ppbv to less than 1 ppbv with a nearly constant loss rate of 0.55 ppbv/h (6.5 hours later, ozone has been completely destroyed). The ozone production is dominated by the photolysis of bromine oxide (R10) and the photolysis of OClO (R15), which is about 20% of the former. The photolysis of chlorine oxide is of no importance. The ozone destruction is dominated by reaction with bromine atoms (R3). Chlorine (R11) contributes 10–15% to the ozone destruction. In total, chlorine is not very effective in destroying ozone, since the ozone production via (R15) comes up to 85–90% of the ozone destruction via (R11). Hence the net ozone destruction of chlorine atoms is just 10–15%.

Therefore we concentrate on the do nothing cycle of (R3) and (R10). Figure 10 shows the cumulated ozone production and destruction by these reactions since the injection of the halogen molecules into the model box. It becomes obvious that this cycle cannot be neglected. The data indicate that in ozone-depleted air masses (O_3 < 20 ppbv), 35–45% of the BrO formed in (R3) have been photolyzed to yield ozone and bromine again. Thus the net ozone destruction of bromine atoms lies between 55 and 65%. To estimate the ozone change and its uncertainty for selected ozone depletion periods from the integrated halogen atom concentrations, we used net ozone destruction potentials of 60 ± 10% for bromine and 10 ± 5% for chlorine (Table 6).

In all cases the chlorine-atom-induced ozone change is of the order of 1% or less. For major ozone depletions as observed on May 4, 5, 6, and 13, 1996, a bromine-atom-induced ozone change of more than 92% is calculated. Hence the total ozone change is obviously dominated by the presence of significant levels of bromine atoms. For major ozone depletions these estimates are in good agreement with the measured ozone changes during those depletions. This means that major ozone depletions can be explained quantitatively using the concept of integrated halogen atom concentrations described here. Even for the May 5–9 period, where the uncertainty of the integrated chlorine atom concentration is larger (see dis-

Table 6. Mean Integrated Halogen Atom Concentrations and Estimated Ozone Changes for Selected Ozone Depletion Periods

Episode in 1996	$\int [Cl \cdot] dt$, 10^9 s cm^{-3}	$\int [Br \cdot] dt$, 10^{12} s cm^{-3}	Ozone Change/%			
			Cl Induced	Br Induced	Cl + Br Effect	Observed
April 1	2.0 ± 0.3	2.1 ± 0.2	0.2 ± 0.1	57.6 ± 23.5	57.7 ± 23.4	53.3
April 26	4.9 ± 0.5	0.2 ± 0.2	0.5 ± 0.2	6.8 ± 38.6	7.2 ± 38.4	27.8
May 2	6.6 ± 1.4	1.9 ± 0.7	0.6 ± 0.3	53.5 ± 31.1	53.8 ± 30.9	67.8
May 4	12.4 ± 1.8	6.4 ± 0.9	1.2 ± 0.6	92.5 ± 11.0	92.6 ± 10.9	98.3
May 5	11.0 ± 1.3	10.5 ± 0.6	1.1 ± 0.5	98.6 ± 3.0	98.6 ± 3.0	100.0
May 6	6.3 ± 4.2	10.8 ± 2.1	0.6 ± 0.5	98.8 ± 2.7	98.8 ± 2.7	99.1
May 8	4.4 ± 4.0	4.6 ± 2.0	0.4 ± 0.4	84.8 ± 18.4	84.9 ± 18.3	86.0
May 13	11.3 ± 2.4	11.4 ± 1.2	1.1 ± 0.6	99.0 ± 2.2	99.0 ± 2.2	97.6

The estimate is based on a net ozone destruction of 60 ± 10% for bromine and 10 ± 5% for chlorine atoms. The error of the estimated ozone changes includes only the errors of the time integrated halogen atom concentrations and the uncertainties of the net ozone destruction potentials. The errors of the rate constants for the reactions of ozone with chlorine or bromine atoms were not considered.

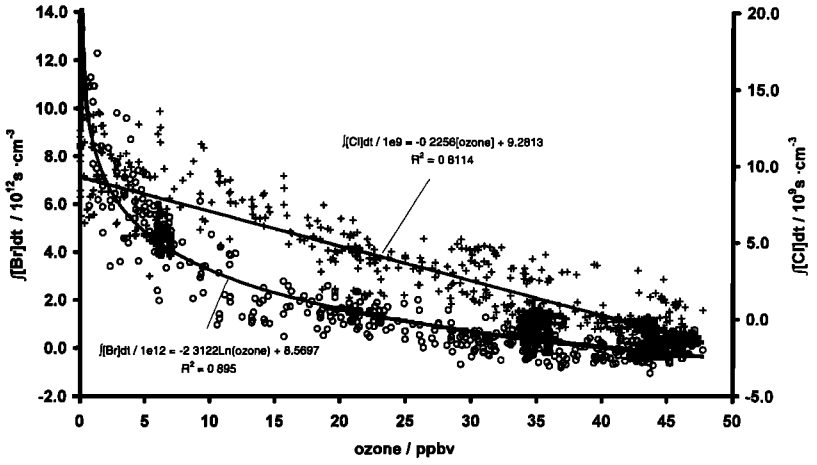

Figure 11. Plot of the integrated halogen atom concentrations versus the ozone mixing ratio. Open circles, $\int$ [Br] dt; crosses, $\int$ [Cl] dt.

cussion above), the estimated (May 6 98.8%, May 8 84.9%) and the observed ozone changes (May 6 99.1%, May 8 86.0%) are still in very good agreement.

For minor ozone depletion events the calculated ozone changes become more uncertain. 57.7 ± 23.4%, 7.2 ± 38.4%, and 53.8 ± 30.9% were calculated for April 1, April 26, and May 2, 1996, respectively. The observed changes for these periods were 53.3, 27.8, and 67.8%, respectively. The agreement between observed and calculated ozone changes is not as good as for the major ozone depletion periods, but the difference can be fully accounted for by the error in the time integrated bromine atom concentration.

4.7. Correlation Between Integrated Halogen Atom Concentrations and Ozone

In principle, the correlation between the integrated halogen atom concentrations and ozone can be derived from (1) and (2) and the relationship between ozone and alkanes or ethyne. The latter can simply be described by a linear function (see Table 4 and discussion thereafter; [*Ramacher*, 1997; *Solberg et al.*, 1996]). Assuming that the initial concentrations $[\text{alkane}]_0$ and $[\text{ethyne}]_0$ are constant for the period of the depletion event, the integrated halogen atom concentrations are proportional to the logarithm of the measured hydrocarbon concentrations. Hence a logarithmic relationship between the time integrated halogen atom concentrations and the ozone mixing ratio should be expected:

$$\int [\text{Cl}]\,dt \sim \ln [\text{alkane}]_x \wedge [\text{alkane}]_x \sim [\text{O}_3] \Rightarrow \int [\text{Cl}]\,dt \sim \ln [\text{O}_3]$$

$$\int [\text{Br}]\,dt \sim \ln [\text{ethyne}]_x \wedge [\text{ethyne}]_x \sim [\text{O}_3] \Rightarrow \int [\text{Br}]\,dt \sim \ln [\text{O}_3]$$

Figure 11 shows a plot of the integrated halogen atom concentrations versus the ozone mixing ratio. Whereas the relationship between the integrated bromine atom concentration and the ozone mixing ratio can be well represented by a logarithmic regression, the relationship between the time integrated chlorine atom concentration and ozone is described best by a linear function. It has to be mentioned that this finding was made independent of the alkane used to derive the integrated chlorine atom concentration.

We believe that the reason for this surprising behavior lies in the missing linear relationship between integrated Cl and integrated Br concentrations (see foregoing discussion). Together with the strong coupling between ozone and Br atoms (more than 98% of the observed ozone loss is caused by Br), the dependency between integrated Cl atom concentration and ozone becomes nonlogarithmic.

5. Summary and Conclusion

During the ARCTOC 96 field campaign, we obtained a unique data set of organic trace gas concentrations in the spring arctic troposphere. The observed changes in the NMHC mixing ratios during low-ozone events confirm previous observations and give evidence for the presence of high concentrations of halogen atoms during these episodes. The hydrocarbon data can be used to calculate integrated halogen atom concentrations of up to 1.4×10^{10} (Cl) and 1.4×10^{13} s cm^{-3} (Br). According to that calculation, ozone is mainly depleted due to bromine-atom-induced chemistry, whereas Cl plays a minor role in ozone destruction. However, Cl is the main cause for the concurrent NMHC depletion. All these findings are in agreement with earlier estimates.

Additionally, the high sampling frequency and the quality of the data allowed us to derive detailed time series of integrated halogen concentrations. On the basis of this evaluation, we made some interesting findings. During a major ozone depletion period between May 5 and 9, 1996, data from ozone soundings and the time integrated chlorine atom concentrations calculated on the basis of different alkanes indicate mixing between air masses that were depleted in ozone to a different extent. Furthermore, the correlation between the integrated chlorine and bromine atom concentrations and their correlation to the ozone mixing ratio were found to be different from general expectations. Although the explanations given here have to be examined in a separate modeling study, we believe that this data set will be very helpful to increase our current understanding of the ozone depletion periods and may give some insight into the mechanism that liberates the halogens.

Acknowledgments. This work was supported by EU grant EV5V-CT93-0318. We thank Norbert Schmidbauer, Sverre Solberg (NILU, Kjeller, Norway), Thomas Arnold (MPI, Mainz, Germany), Gert Koenig-Langlo (Alfred-Wegener-Institut, Bremerhaven, Germany), and Alix Rasmussen (DMI, Copenhagen, Denmark) for providing some of their data. We appreciate the support of Jan Wasseng (NILU), Sverre Thom, Stig Osdal, and Aanon Grimnes (Norsk Polarinstitutt, Ny Ålesund, Svalbard) during the ARCTOC field measurements.

References

Ackermann, R., M. Tuckermann, and U. Platt, DOAS measurements during the ARCTOC campaigns 1995 and 1996 in Ny-Ålesund, Spitsbergen, Atmospheric Research in Ny-Ålesund: Proceedings From the 3rd Nysmac Meeting, *NILU Publ. OR 19/97*, edited by I. Fløisand et al., pp. 131–136, Norw. Inst. for Air Res., Kjeller, 1997.

Ackman, R. G., Fundamental groups in the response of flame ionization detectors to oxygenated aliphatic hydrocarbons, *J. Gas Chromatogr.*, *2*, 173–179, 1964.

Anlauf, K. G., R. E. Mickle, and N. B. A. Trivett, Measurement of ozone during Polar Sunrise Experiment 1992, *J. Geophys. Res.*, *99*, 25,345–25,353, 1994.

Ariya, P., Studies of tropospheric halogen chemistry: Laboratory and field measurements, Ph.D. thesis, York Univ., North York, Ontario, Canada, May 1996.

Ariya, P., V. Catoire, R. Sander, H. Niki, and G. W. Harris, Trichloroethene and tetrachloroethene: Tropospheric probes for Cl and Br atom reactions during the polar sunrise, *Tellus, Ser. B*, *49*, 583–591, 1997.

Arnold, T., M. Martinez-Walter, D. Perner, and R. Seuwen, Peroxy radical behavior during ARCTOC campaigns at Ny Ålesund, Atmospheric Research in Ny-Ålesund: Proceedings From the 3rd Nysmac Meeting, *NILU Publ. OR 19/97*, edited by I. Fløisand et al., pp. 143–146, Norw. Inst. for Air Res., Kjeller, 1997.

Atkinson, R., Kinetics and mechanisms of the gas-phase reactions of the hydroxyl radical with organic compounds under atmospheric conditions, *Chem. Rev.*, *86*, 69–201, 1986.

Atkinson, R., Gas-phase tropospheric chemistry of organic compounds, *J. Phys. Chem. Ref. Data Monogr.*, *2*, 1–214, 1994.

Atkinson, R., and S. M. Aschmann, Kinetics of the gas-phase reactions of Cl atoms with a series of organics at 296+/−2 K and atmospheric pressure, *Int. J. Chem. Kinet.*, *17*, 33–41, 1985.

Atkinson, R., and S. M. Aschmann, Kinetics of the gas-phase reactions of Cl atoms with chloroethenes at 298+/−2 K and atmospheric pressure, *Int. J. Chem. Kinet.*, *19*, 1097–1105, 1987.

Atkinson, R., D. L. Baulch, R. A. Cox, R. F. Hampson, J. A. Kerr, and J. Troe, Evaluated kinetic and photochemical data for atmospheric chemistry, Supplement III, *J. Phys. Chem. Ref. Data*, *18*, 881–1097, 1989.

Atkinson, R., D. L. Baulch, R. A. Cox, R. F. Hampson, J. A. Kerr, and J. Troe, Evaluated kinetic and photochemical data for atmospheric chemistry, Supplement IV, *J. Phys. Chem. Ref. Data*, *21*, 1125–1568, 1992.

Barnes, I., K. H. Becker, and R. D. Overrath, Oxidation of organic sulphur compounds, in *Tropospheric Chemistry of Ozone in Polar Regions, NATO ASI Ser., Subser. 1, Global Environmental Change*, edited by H. Niki and K. H. Becker, pp. 371–383, Springer-Verlag, New York, 1993.

Barrie, L. A., Arctic air chemistry: An overview, in *Arctic Air Pollution*, edited by B. Stonehouse, pp. 5–23, Cambridge Univ. Press, New York, 1986.

Barrie, L. A., J. W. Bottenheim, R. C. Schnell, P. J. Crutzen, and R. A. Rasmussen, Ozone destruction and photochemical reactions at polar sunrise in the lower Arctic atmosphere, *Nature*, *334*(6178), 134–141, 1988.

Beine, H. J., D. A. Jaffe, D. R. Blake, E. Atlas, and J. Harris, Measurements of PAN, alkyl nitrates, ozone, and hydrocarbons during spring in interior Alaska, *J. Geophys. Res.*, *101*, 12,613–12,619, 1996.

Beine, H. J., D. A. Jaffe, F. Stordal, M. Engardt, S. Solberg, N. Schmidbauer, and K. Holmen, NO_x during ozone depletion events in the arctic troposphere at Ny-Ålesund, Svalbard, *Tellus, Ser. B*, *49*, 556–565, 1997.

Bierbach, A., I. Barnes, and K. H. Becker, Rate coefficients for the gas-phase reactions of bromine radicals with a series of alkenes, dienes, and aromatic hydrocarbons at 298 ± 2 K, *Int. J. Chem. Kinet.*, *28*, 565–577, 1996.

Borken, J., Ozonabbau durch Halogene in der arktischen Grenzschicht: Reaktionskinetische Modellrechnungen zu einem Frühjahrsphänomen, Diploma thesis, Ruprecht-Karls-Univ., Heidelberg, Germany, 1996.

Bottenheim, J. W., Polar sunrise studies, in *Tropospheric Chemistry of Ozone in Polar Regions, NATO ASI Ser., Subser. 1, Global Environmental Change*, edited by H. Niki and K. H. Becker, pp. 41–56, Springer-Verlag, New York, 1993.

Bottenheim, J. W., L. A. Barrie, E. Atlas, L. E. Heidt, H. Niki, R. A. Rasmussen, and P. B. Shepson, Depletion of lower tropospheric ozone during arctic spring: The Polar Sunrise Experiment 1988, *J. Geophys. Res.*, *95*, 18,555–18,568, 1990.

Buskühl, M., Optimierung eines Gaschromatographen und anschließende Bestimmung und Interpretation des Konzentrationsverlaufes von Peroxyacetylnitrat in der Luft während der Messkampagne ARCTOC 95 auf Spitzbergen, Diploma thesis, Westfälische-Wilhelms-Univ., Muenster, Germany, 1996.

DeMore, W. B., S. P. Sander, D. M. Golden, R. F. Hampson, M. J. Kurylo, C. J. Howard, A. R. Ravishankara, C. E. Kolc, and M. J. Molina, Chemical kinetics and photochemical data for use in stratospheric modeling, *JPL Publ.*, *97-4*, Eval. 12, 1997.

Dietz, W. A., Response factors for gas chromatographic analyses, *J. Gas Chromatogr.*, *5*, 68–71, 1967.

Ettre, L. S., Relative response of the flame ionization detector, *J. Chromatogr.*, *8*, 525–530, 1962.

Gautrois, M., Entwicklung und Test einer Diffusionsquelle zur Kalibration von gaschromatographischen Messungen halogenierter Kohlenwasserstoffe in der Atmosphäre, Diploma thesis, Gerhard-Mercator-Univ., Duisburg, Germany, 1996.

Hausmann, M., and U. Platt, Spectroscopic measurement of bromine oxide and ozone in the high arctic during Polar Sunrise Experiment 1992, *J. Geophys. Res.*, *99*, 25,399–25,414, 1994.

Hooshiyar, P. A., and H. Niki, Rate constants for the gas phase reactions of Cl atoms with C_2–C_8 alkanes at T = 296 ± 2 K, *Int. J. Chem. Kinet.*, *27*, 1197–1206, 1995.

Hopper, J. F., B. Peters, Y. Yokouchi, H. Niki, B. T. Jobson, P. B. Shepson, and K. Muthumaru, Chemical and meteorological observations at ice camp SWAN during Polar Sunrise Experiment 1992, *J. Geophys. Res.*, *99*, 25,489–25,498, 1994.

Jobson, B. T., H. Niki, Y. Yokouchi, J. W. Bottenheim, F. Hopper, and R. Leaitch, Measurements of C_2–C_6 hydrocarbons during the Polar Sunrise 92 Experiment, *J. Geophys. Res.*, *99*, 25,355–25,368, 1994.

Kirchner, U., T. Benter, and R. N. Schindler, Experimental verification of gas phase bromine enrichment in reactions of HOBr with sea salt doped ice surfaces, *Ber. Bunsenges. Phys. Chem.*, *101*, 975–977, 1997.

Koenig-Langlo, G., and B. Marx, The Meteorological Information System at the Alfred Wegener Institute, in *Climate and Environmental Database Systems*, edited by M. Lautenschlager and M. Reinke, Kluwer Acad., Norwell, Mass., 1997.

Leibrock, E., Entwicklung eines gaschromatographischen Verfahrens zur Spurenanalytik von oxidierten Kohlenwasserstoffen in Luft, in *Schriftenreihe des Frauenhofer-Instituts Atmosphärische Umweltforschung*, vol. 40-96, Wissenschaftsverlag Dr. W. Maraun, Frankfurt, Germany, 1996.

Li, S.-M., Equilibrium of particle nitrite with gas phase HONO: Tropospheric measurements in the high Arctic during polar sunrise, *J. Geophys. Res.*, *99*, 25,469–25,478, 1994.

Martinez-Walter, M., T. Arnold, and D. Perner, Measurements of halogen compounds, O_3, NO_2, and SO_2 during the ARCTOC campaigns in spring 1995 and 1996, Atmospheric Research in Ny-Ålesund: Proceedings From the 3rd Nysmac Meeting, *NILU Publ. OR 19/97*, edited by I. Fløisand et al., pp. 123–126, Norw. Inst. for Air Res., Kjeller, 1997.

McKeen, S. A., and S. C. Liu, Hydrocarbon ratios and photochemical history of air masses, *Geophys. Res. Lett.*, *20*, 2363–2366, 1993.

Moortgat, G. K., R. Meller, and W. Schneider, Temperature dependence (256–296 K) of the absorption cross sections of bromoform in the wavelength range 285–360 nm, in *Tropospheric Chemistry of Ozone in Polar Regions, NATO ASI Ser., Subser. 1, Global Environmental Change*, edited by H. Niki and K. H. Becker, pp. 359–370, Springer-Verlag, New York, 1993.

Mozurkewich, M., Mechanisms for the release of halogens from sea-salt particles by free radical reactions, *J. Geophys. Res.*, *100*, 14,199–14,207, 1995.

Nicovich, J. M., Kinetics and thermochemistry of the $Cl(^2P_j)$ + C_2Cl_4 association reaction, *J. Phys. Chem.*, *100*, 680–688, 1996.

Nicovich, J. M., K. D. Kreutter, and P. Wine, Kinetics of the reaction of Cl and Br with ozone, *Int. J. Chem. Kinet.*, *22*, 399–414, 1990.

Oltmans, S. J., Surface ozone measurements in clean air, *J. Geophys. Res.*, *86*, 1174–1180, 1981.

Ramacher, B., Messung organischer Spurengase in der arktischen Troposphäre: Hinweise auf einen regionalen halogeninduzierten Ozonabbau, *Ber. 3424*, Forschungszentrum Julich, Julich, Germany, 1997.

Ramacher, B., J. Rudolph, and R. Koppmann, Hydrocarbon measurements in the spring arctic troposphere during the ARCTOC 95 campaign, *Tellus*, *Ser. B*, *49*, 466–485, 1997.

Sander, R., R. Vogt, G. W. Harris, and P. J. Crutzen, Modeling the chemistry of ozone, halogen compounds, and hydrocarbons in the arctic troposphere during spring, *Tellus*, *Ser. B*, *49*, 522–532, 1997.

Scanlon, J. T., and D. E. Willis, Calculation of flame ionization detector relative response factors using the effective carbon number concept, *J. Chromatogr. Sci.*, *23*, 333–339, 1985.

Solberg, S., N. Schmidbauer, A. Semb, and Ø. Hov, Boundary-layer ozone depletion as seen in the Norwegian arctic in spring, *J. Atmos. Chem.*, *23*, 301–332, 1996.

Sternberg, J. C., W. S. Gallaway, and D. Jones, The mechanism of response of flame ionization detectors, in *Gaschromatography*, edited by N. Brenner, J. E. Callen, and M. D. Weiss, pp. 231–267, Academic, San Diego, Calif., 1962.

Tang, T., and J. C. McConnell, Autocatalytic release of bromine from arctic snow pack during polar sunrise, *Geophys. Res. Lett.*, *23*, 2633–2636, 1996.

Taylor, P. H., Z. Jiang, and B. Dellinger, Determination of the gas-phase reactivity of hydroxyl with chlorinated methanes at high temperature: Effects of laser/thermal photochemistry, *Int. J. Chem. Kinet.*, *25*, 9–23, 1993.

Tschuikow-Roux, E., T. Yano, and J. Niedzielski, Reactions of ground state chlorine atoms with fluorinated methanes and ethanes, *J. Phys. Chem.*, *82*, 65–73, 1985.

Tschuikow-Roux, E., F. Faraji, S. Paddison, J. Niedzielski, and K. Miyokawa, Kinetics of photochlorination of halogen (F, Cl, Br) substituted methanes, *J. Phys. Chem.*, *92*, 1488–1497, 1988.

Tuckermann, M., R. Ackermann, C. Gölz, H. Lorenzen-Schmidt, T. Senne, J. Stutz, B. Trost, W. Unold, and U. Platt, DOAS-observation of halogen radical-catalysed arctic boundary layer ozone destruction during the ARCTOC-campaigns 1995 and 1996 in Ny-Ålesund, Spitsbergen, *Tellus*, *Ser. B*, *49*, 533–555, 1997.

Vogt, R., P. J. Crutzen, and R. Sander, A mechanism for halogen release from sea-salt aerosol in the remote marine boundary layer, *Nature*, *383*, 327–330, 1996.

Wallington, T. J., L. M. Skewes, and W. O. Siegl, Kinetics of the gas phase reaction of chlorine atoms with a series of alkenes, alkynes, and aromatics at 295 K, *J. Photochem. Photobiol. A*, *45*, 167–175, 1988.

Warneck, P., *Chemistry of the Natural Atmosphere*, Academic, San Diego, Calif., 1988.

Wessel, S., Troposphärische Ozonvariationen in Polarregionen, *Ber. Polarforschung 224*, Alfred-Wegener-Inst. fur Polar- und Meeresforschung, Bremerhaven, Germany, 1997.

Yokouchi, Y., H. Akimoto, L. A. Barrie, J. W. Bottenheim, K. Anlauf, and B. T. Jobson, Serial gas chromatographic/mass spectrometric measurements of some volatile organic compounds in the arctic atmosphere during the 1992 Polar Sunrise Experiment, *J. Geophys. Res.*, *99*, 25,379–25,389, 1994.

R. Koppmann and B. Ramacher, Institut für Atmosphärische Chemie (ICG-3), Leo-Brandt Strasse, Forschungszentrum Jülich GmbH, D-52425 Jülich, Germany. (b.ramacher@fz-juelich.de)

J. Rudolf, Centre for Atmospheric Chemistry, York University, North York M3J 1P3, Ontario, Canada.

(Received March 17, 1998; revised October 19, 1998; accepted October 21, 1998.)